1

Renal Disease

John W. Stirling[1] and Alan Curry[2]

[1]*Centre for Ultrastructural Pathology, IMVS – SA Pathology, Adelaide, Australia*
[2]*Health Protection Agency, Clinical Sciences Building, Manchester Royal Infirmary, Manchester, United Kingdom*

COPYRIGHTED MATERIAL

1.1 THE ROLE OF TRANSMISSION ELECTRON MICROSCOPY (TEM) IN RENAL DIAGNOSTICS

The ultrastructural examination of renal biopsies has made a significant contribution to our understanding of renal disease and is fundamental to accurate diagnosis. For overall tissue evaluation, light microscopy (LM), immunolabelling and transmission electron microscopy (TEM) are generally combined as an integrated protocol. LM is used to make an assessment of overall tissue morphology and to identify the major pathological processes present. Immunolabelling (preferably using immunofluorescence or by the immunoperoxidase technique) is used to determine the composition and location of glomerular immune deposits. Local practices vary, but an antibody panel can contain antibodies directed against IgG, IgA, IgM, complement (C3, C1q and sometimes C4), κ and λ light chains and albumin. TEM can play a major role when LM and immunolabelling findings are normal, only mildly atypical or equivocal and difficult to interpret, particularly in respect to conditions where there may be similar LM or immunolabelling findings. Thus, the technique is particularly useful in the setting of familial disease where the

Diagnostic Electron Microscopy: A Practical Guide to Interpretation and Technique, First Edition. Edited by John W. Stirling, Alan Curry and Brian Eyden.
© 2013 John Wiley & Sons, Ltd. Published 2013 by John Wiley & Sons, Ltd.

structural abnormalities in the glomerular basement membrane (GBM) cannot be resolved by LM (e.g. Alport's syndrome). TEM can also provide critical information not revealed by the other methodologies to identify underlying primary disease and unexpected concomitant disease. Similarly with immunolabelling, the full classification and staging of deposits require ultrastructural analysis. Some transplant biopsies can also benefit from ultrastructural evaluation (see Chapter 2); however, TEM rarely contributes to the diagnosis of tubular, vascular or interstitial disease. Overall, ultrastructural screening is essential; it can change the diagnosis in ~25% of cases and provides 'useful' information in ~66% of cases (Pearson *et al.*, 1994; Elhefnawy, 2011).

1.2 ULTRASTRUCTURAL EVALUATION AND INTERPRETATION

Examination of glomeruli (and other areas, if necessary) should be thorough and systematic with all components being evaluated for possibly significant features or changes. During screening, a range of representative images should be taken. These should include low-power images to show overall glomerular morphology, plus a representative selection of higher power images to show the specific and critical diagnostic features. In some instances, it may also be important to show that certain features are, in fact, absent (e.g. deposits) or normal (e.g. foot processes). The principal elements that should be examined are (i) the location, size and morphology of immune-related deposits and other inclusions; (ii) the thickness, overall morphology and texture of the GBM; (iii) the size and morphology of the mesangial matrix and (iv) the number and morphology of the cellular components of the glomerulus (Stirling *et al.*, 2000). Sclerotic glomeruli should be avoided, and only well-preserved functional (or significantly functional) glomeruli should be examined. It is also important to ensure that the glomeruli screened are representative of the LM findings: this means that, ideally, the choice of glomeruli to be screened (from semithin sections) should be done in collaboration with the reporting pathologist. Finally, it should be stressed that screening should be unbiased, although some knowledge of the pathology and immunolabelling results may be useful if the features expected are minor or uncommon. The vascular pole should be avoided during ultrastructural evaluation as it may contain misleading nonpathologic deposits, and likewise Bowman's capsule which has no real diagnostic value, although the presence of crescents can be confirmed.

Following evaluation, representative images and findings should be communicated to the reporting pathologist, the latter verbally or in a concise written report. If the initial evaluation does not correspond with the LM evaluation (e.g. the electron microscopy (EM) samples only a tiny fraction of the available tissue), then the specimen should be re-examined or additional glomeruli observed to increase diagnostic confidence.

A critical question is 'How many glomeruli should be examined, and for how long?' Unfortunately, there is no definitive answer to this dilemma except to say that enough tissue should be examined to answer the diagnostic question posed and to ensure that no additional or unexpected pathology is present. A single glomerulus (or even part of one) may be adequate in respect to diffuse disease and/or when the glomerulus screened is typical of the disease process identified by LM. In contrast, several glomeruli, or possibly glomeruli from different blocks, may be required to capture the full range of pathological changes in focal disease. Perhaps the final word on this issue is to say that the tissue must be screened thoroughly; it is bad practice to stop screening once the features that were expected have been located because additional findings that affect the accuracy of the diagnosis may be missed.

1.3 THE NORMAL GLOMERULUS

The glomerulus (Figure 1.1) is composed of a tuft of branching capillaries that originate from the afferent arteriole at the vascular pole to form a series of lobules (segments) that ultimately rejoin at the vascular pole and exit the glomerulus via the efferent arteriole. At the core of each lobule is the mesangium which supports the capillary loops; capillary loops are lined by endothelial cells (Figure 1.1). The mesangial matrix principally consists of collagen IV and is populated by mesangial cells (usually 1–3 in normal mesangium) plus a small number of immune-competent cells and rare transient cells of the monocyte–macrophage lineage (Sterzel *et al.*, 1982). The entire capillary tuft is enclosed within Bowman's capsule, the inner aspect of which is lined by a thin layer of epithelial cells (the parietal epithelial cells); a second inner population of epithelial cells (the visceral epithelial cells or podocytes) is closely associated with the capillary tufts, and extensions of these cells form the foot processes (pedicels) that cover the outer aspect of the capillary walls (Figure 1.1). The podocytes are the sole source of the collagen IV $\alpha 3$, $\alpha 4$ and $\alpha 5$ subtypes that form the bulk of the GBM (Abrahamson *et al.*, 2009), and the foot processes play a major role in ultrafiltration and the

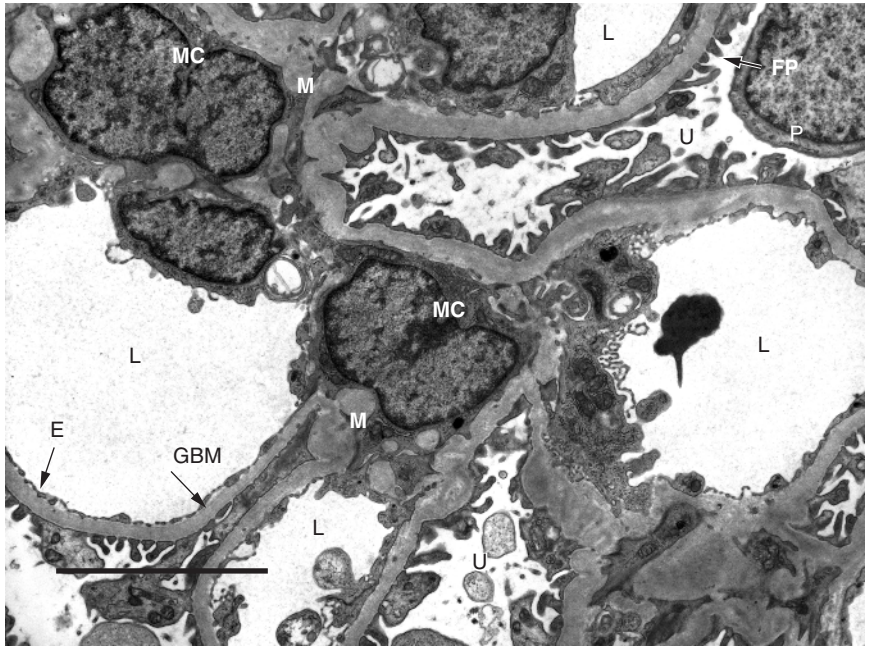

Figure 1.1 Detail of a normal glomerulus. The capillary loops are supported by the mesangium (M). Mesangial cells with nuclei (MC); capillary lumens (L); urinary space (U); podocyte (P) (epithelial cell) and foot processes (FP). Here, the overall width of Overall, the glomerular basement membrane (GBM) averages ~380 nm in width. Loops are lined with fenestrated endothelial cells (E). Bar = 5 μm.

maintenance of the filtration barrier. As a result, podocyte dysfunction plays a major role in a wide range of glomerular diseases (Wiggins, 2007; Haraldsson, Nystrom and Deen, 2008). Opposite the vascular pole, Bowman's capsule is continuous with the proximal tubule which drains filtrate from the glomerulus (the urinary pole). Overall, filtration is said to be a function of size, shape and charge selection, although the nature and contribution of charge selection are debated (Harvey *et al*., 2007; Haraldsson, Nystrom and Deen, 2008; Goldberg *et al*., 2009). The capillary wall as a whole is responsible for the filtration process, and it appears that the capillary endothelium, the GBM and the podocyte foot processes must all be intact for normal filtration to occur (Patrakka and Tryggvason, 2010).

1.3.1 The Glomerular Basement Membrane

The GBM (Figure 1.1) is made of three layers: (i) the lamina rara interna, the electron-lucent layer immediately adjacent to the endothelium;

(ii) the lamina densa, the central layer and (iii) the lamina rara externa, the outer electron-lucent area immediately adjacent to the foot processes. The lamina densa makes up the bulk of the GBM and is its main structural element; it has a felt-like fibrillar construction, and knowledge of its molecular makeup is helpful in understanding and interpreting familial and autoimmune disease. The principal component is collagen IV, which consists of six subtypes ($\alpha1$–$\alpha6$) (Patrakka and Tryggvason, 2010). In the developing kidney, the GBM is initially formed of the $\alpha1$ and $\alpha2$ subtypes with the $\alpha3$, $\alpha4$ and $\alpha5$ subtypes forming later (the additional subtype, $\alpha6$, is restricted to Bowman's capsule and some tubular basement membranes) (Harvey *et al*., 1998; Miner, 1998). In the mature kidney, the $\alpha1$ and $\alpha2$ subtypes are restricted to a narrow band immediately adjacent to the capillary endothelium; the $\alpha3$, $\alpha4$ and $\alpha5$ subtypes form the remaining bulk of the GBM (extending out to the foot processes). The core of the mesangial matrix is composed of the $\alpha1$ and $\alpha2$ subtypes (continuous with the inner aspect of the GBM), while the outer peripheral layer is made up of the $\alpha3$, $\alpha4$ and $\alpha5$ subtypes (continuous with the outer layer of the GBM) (Butkowski *et al*., 1989; Harvey *et al*., 1998; Miner, 1998). The $\alpha3$, $\alpha4$ and $\alpha5$ subtypes are essential for the maintenance of normal glomerular function, and mutations in the genes for these subtypes are responsible for the various forms of membrane-related hereditary nephritis. The structural abnormalities of the GBM in hereditary disease are caused by the absence of the $\alpha3$ and $\alpha5$ subtypes, because without either of these, the membrane fails to form correctly (Kalluri *et al*., 1997; LeBleu *et al*., 2010; Miller *et al*., 2010). The $\alpha3$ subtype has been identified as the Goodpasture epitope (Saus *et al*., 1988). However, it appears that both the $\alpha3$ and $\alpha5$ subtypes are targeted in anti-GBM disease, while in Alport's post-transplantation nephritis, only the $\alpha5$ subtype is involved (Pedchenko *et al*., 2010).

1.4 ULTRASTRUCTURAL DIAGNOSTIC FEATURES

1.4.1 Deposits: General Features

Immune-related material accumulates as discrete or linear deposits of finely granular electron-dense material within or adjacent to the GBM and/or mesangium in several diseases. Deposits may also be 'organised' as tubules and fibrils of various diameters, as crystals and as whorls with a fingerprint-like appearance (Herrera and Turbat-Herrera, 2010). The identity and content of specific deposits vary and must be confirmed by immunolabelling.

Note that scattered deposits may sometimes be an incidental finding with no obvious pathological or diagnostic relevance. Approximately 4–16% of normal individuals have mesangial IgA deposits (without IgG or C3) (Coppo, Feehally and Glassock, 2010), and small numbers of discrete deposits are occasionally seen in individuals with naturally high levels of antigenic challenge.

1.4.2 Granular and Amorphous Deposits

1.4.2.1 Subepithelial Deposits

Subepithelial deposits are finely granular, medium-density deposits located on the outer surface of the GBM and the mesangium. Foot processes that lie over the surface of the deposit are generally effaced.

- Large oval or dome-like deposits (humps). True humps are not usually associated with a GBM reaction (spikes). Seen typically in post-infectious glomerulonephritis (PIGN) (Figure 1.14).
- Flat or nodular deposits. There may be an associated GBM reaction with 'spikes' of new membrane forming adjacent to the deposits, a process that may ultimately lead to the deposits becoming incorporated into the GBM (chain-link appearance by LM). Seen typically in stage I membranous glomerulonephritis (Figure 1.10).

1.4.2.2 Intramembranous Discrete Deposits

These are finely granular, medium-density deposits that lie completely within the lamina densa. The material may be uniform in appearance, or patchy and irregular. Resorption of deposits results in irregular electron-lucent areas surrounded by thickened GBM; badly damaged membrane may become laminated and similar in appearance to the 'basket weave' pattern seen in Alport's syndrome. Seen typically in stage III membranous glomerulonephritis (Figure 1.12).

1.4.2.3 Intramembranous Linear Deposits

- Linear transformation: a uniform dense amorphous transformation of the GBM that results in a dark, 'ribbon-like' appearance. The material is essentially sited within the subendothelial layer of GBM matrix

and may penetrate the GBM for some distance. Seen typically in mesangiocapillary glomerulonephritis (MCGN) type II (dense deposit disease (DDD)) (Figure 1.17). A similar effect may be seen around the periphery of loops when subepithelial deposits merge to form a continuous or semicontinuous band.
- Medium-density linear deposits of finely granular or powdery material within the GBM. Seen typically in κ light-chain disease (Figure 1.21).

1.4.2.4 Subendothelial Deposits

These are linear or plaque-like, finely granular, medium-density deposits located between the inner aspect of the GBM and the capillary endothelium. Large deposits may be visible by LM as nodular hyaline 'thrombi' or as 'wire-loop' capillary wall thickening. Seen typically in MCGN type I (Figure 1.16).

1.4.2.5 Mesangial Deposits

- Mesangial: finely granular, medium-density deposits within the central mesangial matrix. Seen typically in IgA disease (Figure 1.15).
- Paramesangial: finely granular, medium-density deposits around the outer periphery of the mesangial matrix, especially at the junction of the capillary loop and the mesangium. Seen typically in IgA disease (Figure 1.15).

1.4.3 Organised Deposits: Fibrils and Tubules

Many normal and pathological fibrils are found in the glomerulus, and the deposition of proteins, such as monoclonal immunoglobulins or their light-chain or heavy-chain subunits, can produce several glomerular diseases (see reviews by Furness, 2004; Basnayake *et al.*, 2011). The accurate identification of fibrils can be problematic, and distinguishing between normal and pathological types may require the correlation of ultrastructural, immunolabelling and LM-staining characteristics (Table 1.1). A number of algorithms have been published to aid in the diagnosis of renal diseases containing organised deposits (Figure 1.2) (see Ivanyi and Degrell, 2004; Herrera and Turbat-Herrera, 2010).

Table 1.1 Characteristics of immune and non-immune glomerular fibrils.

Fibril type	Characteristics
Amyloid (Figure 1.22)	**Transmission electron microscopy (TEM) characteristics** Extracellular nonbranching fibrils Random orientation, occasionally in parallel arrays Fibrils may appear to penetrate, or flow (cascade) from, adjacent cells Distribution diffuse or focal; includes GBM Diameter: ~7–10 nm (Ghadially, 1988) or ~8–12 nm (Rosenstock *et al*., 2003) **Light microscopy (LM) characteristics** Periodic acid–Schiff (PAS) negative; non-argyrophilic Congo red positive (also Sirius red and Thioflavin T and S positive in fresh tissue) Positive Congo red reaction requires a reasonable amount of amyloid to be present. Sections should be 8–10 μm thick. Apple green birefringence under polarised light (Vowles, 2008). **Immunolabelling** Negative for immunoglobulins, complement components, fibrinogen and albumin. Composition variable. Immunolabelling may be used to identify precursor proteins in order to identify amyloid type (Vowles, 2008).
'Immune' fibrils (fibrillary glomerulonephritis) (Figure 1.23)	**TEM characteristics** Extracellular nonbranching fibrils Random, sometimes parallel orientation Distribution diffuse; includes GBM Diameter: 13–29 nm (mean 20.1 nm ±0.4) (Rosenstock *et al*., 2003) or 15–25 nm (Herrera and Turbat-Herrera, 2010) **LM characteristics** Glassy and weakly eosinophilic; weakly PAS positive; grey-purple on trichrome stain; non-argyrophilic (Rosenstock *et al*., 2003) PAS–methenamine–silver: weak (reticular) staining Congo red negative **Immunolabelling** Smudgy, ribbon-like to granular staining for IgG, C3 and κ and λ light chains (sometimes with light-chain restriction) in mesangium and peripheral capillary walls. IgG4 is dominant in most cases, but rarely IgG1 (Herrera and Turbat-Herrera, 2010).

Table 1.1 (*continued*)

Fibril type	Characteristics
Immunotactoid glomerulopathy ('immune' tubules) (Figure 1.24)	**TEM characteristics** Extracellular nonbranching tubules Orientation random, or in parallel arrays; sometimes in a background matrix (Herrera and Turbat-Herrera, 2010 Distribution diffuse; includes mesangium and GBM Diameter: 20–55 nm (mean 38.2 nm ± 5.7) (Rosenstock *et al*., 2003) or 10–90 nm (commonly more than 30 nm) (Herrera and Turbat-Herrera, 2010) **LM characteristics** Silver stains negative **Immunolabelling** Variable, IgG and C3 in mesangium and peripheral capillary walls with a granular or pseudolinear pattern; IgA, IgM and C1q variable or negative; light-chain restriction (κ rather than λ) in some cases (Herrera and Turbat-Herrera, 2010)
Microfibrils	**TEM characteristics** Extracellular nonbranching fibrils Parallel, 'bundled' or sometimes random orientation Normal microfibrillar glomerular components include (i) collagen fibrils ~30 nm in diameter and greater; (ii) 'large' fibrils ~18–20 nm in diameter; (iii) 'small' fibrils ~10 nm in diameter and (iv) 'thin filaments' ~3–5 nm in diameter (Coleman and Seymour, 1992). Nonspecific fibrils ~12 nm in diameter may be found in several conditions, especially sclerosing glomerular diseases (Hsu and Churg, 1979; Kronz, Nue and Nadasdy, 1998). 12 nm diameter non-immune fibrils are a major component of Kimmelstiel–Wilson nodules (Figure 1.8) (Yasuda *et al*., 1992). **LM characteristics** Generally PAS and PAS–methenamine–silver strongly positive Congo red negative **Immunolabelling** Negative or nonspecific (Kronz, Nue and Nadasdy, 1998)

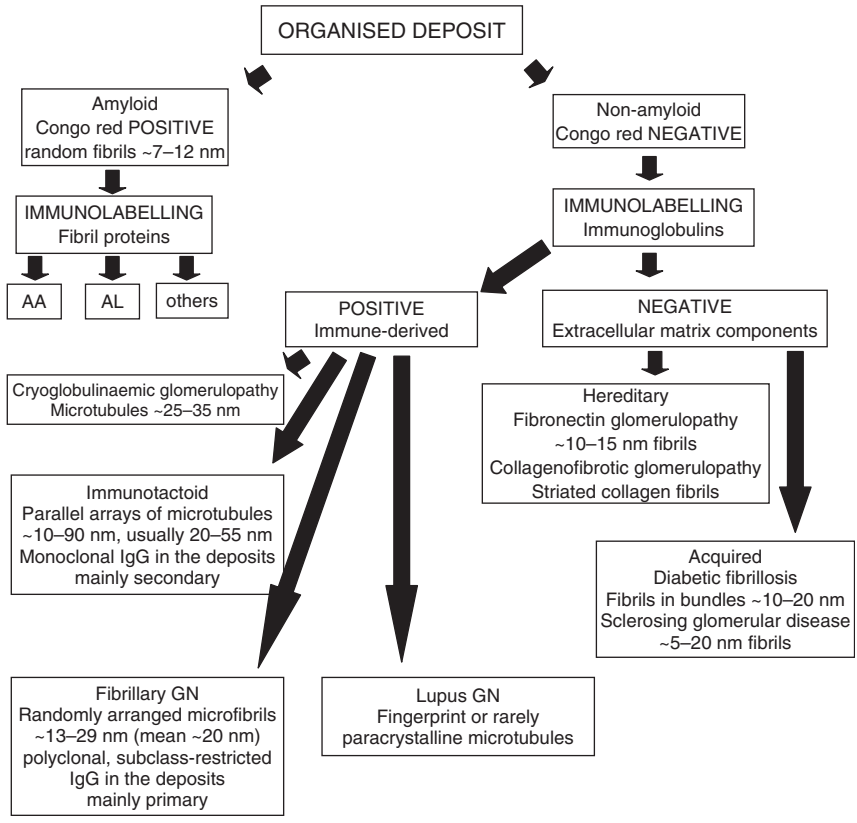

Figure 1.2 Algorithm for diagnosis of organised deposits. An algorithm to aid in the diagnosis of diseases with organised deposits (based on Ivanyi and Degrell, 2004; Herrera and Turbat-Herrera, 2010). Measurements given are fibril and tubule diameters (see Table 1.1 for source references). This strategy may be combined with silver methenamine staining to further define matrix-derived components (Herrera and Turbat-Herrera, 2010).

1.4.3.1 Amyloid

Amyloid is composed of insoluble fine fibrils made up of low-molecular-weight proteins of various types in a β-pleated sheet conformation (Dember, 2006; Vowles, 2008). Amyloid deposits may form anywhere in the glomerulus (and other tissues) as extracellular nonbranching fibrils of indeterminate length and without cross-striations (Table 1.1; Figure 1.22). Immunofluorescence can sometimes indicate the possibility

of amyloid deposition (dull green colouration), but this can be difficult to differentiate from diabetic changes (increase in matrix).

1.4.3.2 Non-amyloid Fibrils and Tubules

Both fibrils and tubules of immune-related material may be found in glomeruli; they may be randomly orientated or organised in parallel arrays. Reported diameters for both fibrils and tubules vary greatly, presumably because of their individual physiochemical makeup, the range of cases sampled and variability in laboratory processing regimes (Table 1.1). Fingerprint deposits (parallel or linear arrays of fibrils – usually curved in a fingerprint-like pattern; Figure 1.20) may also be found, particularly in systemic lupus erythematosus (SLE) and cryoglobulinaemia. There is some dispute as to whether diseases featuring immune fibrils (fibrillary glomerulonephritis; Figure 1.23) and those featuring tubules (immunotactoid glomerulopathy; Figure 1.24) should be treated together or separately (Schwartz, Korbet and Lewis, 2002; Ivanyi and Degrell, 2004; Herrera and Turbat-Herrera, 2010). Here, they are treated as separate entities as there are important clinical differences between them, that is, immunotactoid is normally associated with a lymphoproliferative disorder, but typically, fibrillary glomerulonephritis is not.

1.4.4 Nonspecific Fibrils

A variety of nonspecific fibrils that may be confused with immune deposits have been found in glomeruli (see Herrera and Turbat-Herrera, 2010; and review by Coleman and Seymour, 1992). Some normal matrix components may be more prominent in pathological conditions. Mesangial microfibrils may be particularly well developed in MCGN and diabetic glomerulosclerosis (Table 1.1). Fibrillar collagen is found within the GBM in nail–patella syndrome (Coleman and Seymour, 1992).

1.4.5 General and Nonspecific Inclusions and Deposits

Several nonspecific inclusions such as microparticles (small electron-dense granules), fibrils and membrane-like material may be found within

the GBM and mesangial matrix – mostly with doubtful or unknown diagnostic significance. Most common are accumulations of spherical particles and vesicles (often referred to as inclusions or virus-like particles): these may be found in the mesangium but are often seen in a subepithelial location, especially in the angle (or 'notch') between two adjoining capillary loops. Microparticles are sometimes seen in areas of laminated GBM in Alport's syndrome (Figure 1.5); similar granules are also found in thickened loops in diabetic sclerosis. Local accumulations of moderately electron-dense material similar to immune-related deposits may be observed, most commonly in a subendothelial location. In the absence of positive immunolabelling, these may relate to the insudation of plasma proteins and/or the development of 'fibrin' caps.

1.4.6 Fibrin

Fibrin may be present in numerous diseases in almost any location in the glomerulus. It may be found as irregular, angular or needle-like accumulations of amorphous material of medium electron density, or it may show cross-striations with a characteristic periodicity. The periodicity of normal fibrin is reported as 22.5 nm (Standeven, Ariëns and Grant, 2005); however, periodicities of ~19–35 nm are reported in pathological tissues in general (Ghadially, 1988). Fibrin is easily distinguished from fibrillar collagen which has an axial banding periodicity of 64–68 nm.

1.4.7 Tubuloreticular Bodies (Tubuloreticular Inclusions)

Tubuloreticular bodies (TRBs) are small clusters of fine anastomosing tubules that arise within the cisternae of the rough endoplasmic reticulum; in the glomerulus, they are most commonly found in endothelial cells (Figure 1.18b). The formation of TRBs has been linked to α- and ß-interferon activity (Hammar *et al*., 1992). In renal disease, TRBs are most commonly associated with SLE (Figure 1.18b) (and collagen vascular diseases in general), with viral infections (especially HIV/AIDS and hepatitis B) and as a result of α-interferon treatment (Hammar *et al*., 1992; Haas *et al*., 2000; Haas, 2007; Yang *et al*., 2009b). However, TRBs are not specific to these conditions as they have also been found in renal transplants and have been linked to diabetes, lymphoma and *Helicobacter pylori* infection (Yang *et al*., 2009b). The presence of TRBs in idiopathic conditions can act as an indicator of underlying systemic

disease, and their presence should prompt additional investigations (Yang *et al*., 2009b).

1.4.8 The Glomerular Basement Membrane

1.4.8.1 GBM Width

Reported measurements for adult GBM vary greatly, but mean widths generally fall in the range of 300–400 nm (Figure 1.1) (see Coleman *et al*., 1986; review by Dische, 1992; Bonsib, 2007). The GBM of children is reported as being slightly thinner up to age 9 (Morita *et al*., 1988). A review by Marquez *et al*. (1999) found that in addition to the variability in values reported for GBM width in adults, there are conflicting data regarding age- and sex-related differences: some studies indicate that the GBM in males and females is similar, but in others, males are said to have slightly thicker GBM than females. Similarly, some studies suggest that the GBM continues to increase in width with age, whereas others do not. Overall, this variation is presumed to reflect the type of tissue used to obtain 'normal' data, the differing morphometric techniques employed and the variation inherent in tissue processing and choice of reagents (Marquez *et al*., 1999; Edwards *et al*., 2009). With these variations in mind, it is clear that statements about GBM width must be treated with caution. For measurements to be meaningful, a set of normal values must be established based on local processing methodology.

1.4.8.2 Thickness, Texture and General Morphology

- **Thickness**: the GBM may be:
  - **Thin**: the membrane may be evenly thinned to ~20–30% of normal width (±100 nm) (Figure 1.6).
  - **Thickened**: the membrane may be evenly thickened up to four times normal width or more (±1000 nm or more) (Figure 1.7).
  - **Irregular**: the membrane may be highly irregular in thickness, although the overall mean may be close to normal (Figure 1.5).
- **Texture**: the GBM may appear to be split or laminated. Lamination may be irregular with a 'basket weave pattern' (Figure 1.5). Small areas of irregular lamination combined with poorly defined electron-lucent areas may be caused by the resorption of deposits.

Faint circumferential lamination is sometimes seen in thickened loops in diabetic glomerulosclerosis.

- **Folding:** loops may become folded or show concertina-like wrinkling as a result of ischaemic collapse. Folds may consolidate to form a thickened area of GBM in which the original folds remain visible. Similar folding may be seen around the periphery of the mesangium (Figure 1.4).
- **Double contouring (interposition):** the GBM becomes duplicated. The duplication is caused by the interposition of mesangial and inflammatory cells, matrix and (in some cases) deposits between the original GBM and the endothelium with the eventual formation of a new inner (luminal) layer of basement membrane material ('tram-tracking' by LM) (Figure 1.16).
- **Subendothelial widening:** the endothelium and the GBM may become separated with the formation of a subendothelial space filled with flocculent material (Figure 1.9) or, more rarely, microfibrils and cellular elements from the blood.
- **Gaps:** small breaks are sometimes seen in the GBM. Despite speculation that these are linked to haematuria, breaks are rare, even in cases of macroscopic haematuria.

1.4.9 The Mesangial Matrix

The principal pathological change seen in the mesangium is enlargement of the extracellular matrix, a process that may lead to the obliteration of part or all of the glomerulus (sclerosis). Matrix expansion may be accompanied by an increase in cellularity, immune-related deposits and several nonspecific inclusions such as microfibrils and granular and/or vesicular material. Rarely, the mesangium may be dissolved or attenuated (mesangiolysis) so that the capillary loops are able to fuse and expand (Morita and Churg, 1983).

1.4.10 Cellular Components of the Glomerulus

1.4.10.1 Capillary Endothelium

Endothelial swelling and hypercellularity may occur in many conditions. Significant numbers of TRBs may be found in several conditions and may contribute to the identification and understanding of underlying pathology (Yang *et al.*, 2009b).

1.4.10.2 Epithelium

1.4.10.2.1 Visceral Epithelium (Podocytes)

In proteinuric diseases, the normal structure and arrangement of the podocyte foot processes are often lost: this occurs when the actin cytoskeleton is reorganised, and the processes merge to form a continuous or semicontinuous cytoplasmic layer (foot process effacement, obliteration or fusion) (D'Agati, 2008; Haraldsson, Nystrom and Deen, 2008). Numerous cytoplasmic inclusions are found in podocytes, most notably lysosomes, lipid vesicles and protein droplets. Abnormal lysosomes may be present because of an inherited storage disorder such as Fabry's disease or as a result of drug treatment (e.g. amiodarone and gold therapy). Podocytes may develop numerous long microvilli in a process known as microvillous transformation (Figure 1.3).

1.4.10.2.2 Parietal Epithelium

The parietal epithelium may proliferate to form cellular 'crescents' that range from small groups of cells to large masses that completely surround

Figure 1.3 Minimal change disease. Foot processes are almost completely effaced (foot process effacement), (FPE). The podocyte (P) contains several vesicles, some of which contain lipid (V); there is also significant microvillous transformation (MV). The glomerular basement membrane (GBM) is slightly thin (190 nm in the thinnest areas). L = capillary lumen. Bar = 5 μm.

the capillary tuft. Fibrin and inflammatory cells such as polymorphs and macrophages may be intermingled with the proliferating cells; in older crescents, fibroblasts and myofibroblasts may also be present. Crescents are nonspecific and a marker of significant glomerular damage; some degree of scarring always remains. At the urinary pole, the junction of the columnar epithelium of the proximal tubule and the parietal epithelial cells is normally sharply marked. Rarely, the tubular epithelium encroaches into the glomerulus, replacing the parietal epithelium in the immediate vicinity of the tubule (termed tubularisation).

1.4.10.3 Mesangial Cells

Mesangial cells proliferate in a number of conditions; this may be accompanied by matrix expansion.

1.4.11 The Capillary Lumen

The capillary lumen may be partially or wholly occluded (stenosed) because of the presence (or effect) of immune-related deposits, insudate, mesangial interposition, endothelial swelling, infiltrating inflammatory cells, capillary wall collapse and/or GBM thickening or folding. Fibrin tactoids and platelets may also be present. On rare occasions, tubular epithelial cells and cell fragments may be found within capillary loops (and the urinary space) – presumably a biopsy artefact.

1.5 THE ULTRASTRUCTURAL PATHOLOGY OF THE MAJOR GLOMERULAR DISEASES

1.5.1 Diseases without, or with Only Minor, Structural GBM Changes

1.5.1.1 Minimal Change Disease (Minimal Change Nephrotic Syndrome or Lipoid Nephrosis)

Minimal change disease (MCD) is a diagnosis based on morphological features, clinical presentation (nephrotic syndrome) and response to therapy (steroid responsive). Primary disease appears to be linked to T-cell dysfunction and type 2 cytokines, while secondary disease results from

a wide range of neoplasms, infections, allergens and drugs (Glassock, 2003; Grimbert *et al*., 2003; Mathieson, 2003).

By LM, the glomeruli appear normal. The most significant ultrastructural feature is foot process effacement, which generally affects greater than 75% of the capillary loop surface (Figure 1.3). Foot process effacement is reversible so that during treatment, only partial effacement or 'smudging' may be observed. Podocytes may contain cytoplasmic vesicles and show significant microvillous transformation (Figure 1.3). Occasionally, mesangial cellularity may be slightly increased. There are no other significant pathological features except that the GBM may be slightly thin (Figure 1.3) (Coleman and Stirling, 1991). Immunolabelling is negative except for weak localised mesangial positivity for IgM and C3 that may indicate segmental sclerosis.

1.5.1.2 Focal Segmental Glomerulosclerosis

Focal segmental glomerulosclerosis (FSGS) is a term that covers five histopathological variants as defined by the Columbia classification (collapsing, glomerular tip lesion, cellular, perihilar and not otherwise specified) which can be applied to both primary and secondary disease (D'Agati *et al*., 2004). In addition to primary (idiopathic) disease, FSGS has a wide variety of causes including mutations in podocyte proteins, viral infections, toxins and drugs; it can also result from adaptive structural-functional responses in association with numerous insults (D'Agati *et al*., 2004). The disease recurs in ~20–30% of grafts, and there is a poor graft survival rate in patients with recurrent disease (Ponticelli, 2010). Historically, FSGS has been grouped with MCD, and it has been argued that primary FSGS is an autoimmune T-cell-driven disease – a concept that is increasingly out of favour. To date, no T-cell association or circulating permeability factor has been found, and the true nature of the underlying pathophysiology of primary nephrotic FSGS remains elusive (Meyrier, 2009).

FSGS is characterised by segmental sclerosis caused by expanding mesangial matrix with capillary loop folding and collapse that lead to progressive consolidation. Foot processes are extensively effaced in sclerosing areas with >50% effacement of capillary loop foot processes elsewhere (in secondary disease, there may be <50% effacement) (Figure 1.4). In some cases, the foot processes may be completely lost so that the outer surface of the GBM is exposed; in such areas,

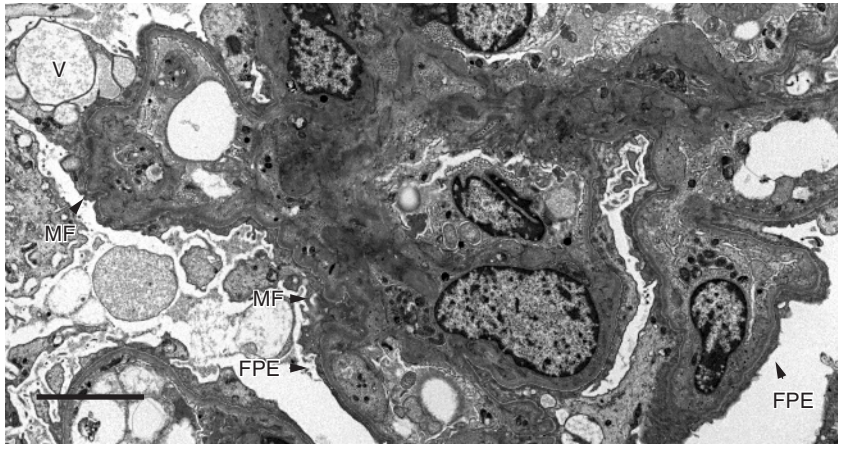

Figure 1.4 Focal segmental glomerulosclerosis. Foot processes are extensively effaced (FPE) with no intact processes remaining, and podocytes contain large vesicles with a variety of appearances (V). Microvillous change and mesangial consolidation are not prominent in this example, but areas of glomerular basement membrane and peripheral mesangium are folded and consolidated, presumably because of ischaemic collapse (MF). Bar = 5 μm.

the underlying matrix may be patchy or laminated in appearance. The podocytes often show significant microvillous transformation and may contain large numbers of cytoplasmic vesicles of varying density (Figure 1.4). In advanced disease, there may be collections of spherical particles and vesicles plus electron-dense granular deposits within the affected segments, as well as large areas of dense material corresponding to the hyaline seen by LM. There may be foam cells present in the glomerular tip lesion and cellular variants, and in the collapsing variant, the capillary loops may be folded, wrinkled and collapsed. In HIV-associated nephropathy, which mainly presents as the collapsing variant, there are generally numerous TRBs in endothelial cells. Immunolabelling generally shows reactions for IgM and C3 in segmental lesions and irregular masses corresponding to hyaline deposits. Diffuse mesangial positivity for IgM and C3 is seen in HIV-associated nephropathy. Nonsclerotic segments may also show some IgM positivity.

1.5.1.3 Pauci-Immune Glomerulonephritis (ANCA-Associated Glomerulonephritis)

Pauci-immune crescentic glomerulonephritis is the most common form of crescentic disease (50–60% of cases). Approximately 80–90% of patients have circulating anti-neutrophil cytoplasmic antibodies

(ANCA). By light and electron microscopy, pauci-immune and anti-GBM glomerulonephritis are similar (see Section 1.5.1.4). Some ANCA-positive cases may show positive immunolabelling and/or electron-dense deposits: these represent concurrent anti-GBM disease (linear labelling) or immune-complex mediated disease (granular labelling and electron-dense deposits), respectively (Rogers, Rakheja and Zhou, 2009). As vascular injury progresses, loops may show endothelial swelling with the development of a subendothelial lucent zone and fibrin deposition; there may also be breaks in the GBM and loss of mesangial matrix, also with fibrin deposition.

1.5.1.4 Anti-GBM Glomerulonephritis (Goodpasture Syndrome)

Anti-GBM disease is characterised by rapidly progressive glomerulonephritis with two peaks of onset, the first at 20–30 years with a male preponderance and a second at 50–70 years with a female preponderance. The disease is linked to cigarette smoking and exposure to hydrocarbons. The target antigens of the circulating autoantibodies are principally the noncollagenous NC1 domains of collagen IV $\alpha 3$ and, to a lesser extent, collagen IV $\alpha 5$. Antibodies to $\alpha 3$ generally appear first, followed by a gradual increase in antibodies to $\alpha 5$ (Pedchenko *et al.*, 2010). Ultimately, antibodies may develop that react with all of the $\alpha 1$–$\alpha 5$ subtypes (Zhao *et al.*, 2009; Pedchenko *et al.*, 2010). High levels of circulating autoantibodies and the presence of antibodies against a broad range of collagen IV subtypes are associated with more severe disease (Yang *et al.*, 2009a; Zhao *et al.*, 2009).

LM shows widespread crescents (often more than 80%) and focal segmental necrotising glomerulonephritis with infiltrating neutrophils. There are no distinct diagnostic ultrastructural features of anti-GBM disease beyond those of necrotising glomerulonephritis: there may be breaks in the GBM, segmental necrosis and inflammatory cells in capillary loops. Fibrin within necrotic areas may mimic electron-dense deposits. Immunolabelling shows diffuse, global, linear staining for IgG; some IgM, IgA and C3 may also be present.

1.5.2 Diseases with Structural GBM Changes

1.5.2.1 Alport's Syndrome

Alport's syndrome is a progressive, genetically and phenotypically diverse disease that affects ~1 : 50 000 live births (Levy and Feingold,

2000). The predominant form is X linked; however, there are also autosomal recessive and autosomal dominant forms (Jais *et al*., 2000, 2003; Hudson *et al*., 2003). The mutations involved result in defective basement membrane assembly that affects renal function and causes deafness, ocular changes and leiomyomatosis. The X-linked form (~80% of cases) is associated with a large number of mutations in the collagen IV $\alpha 5$ gene (Barker *et al*., 1990; Martin *et al*., 1998). Affected individuals show microscopic haematuria, proteinuria (with or without nephrotic syndrome) and hypertension; progressive renal failure develops in males. A small number of males (~2.5%) develop anti-GBM glomerulonephritis on transplantation (Jais *et al*., 2000; Adler and Salant, 2003). Female carriers generally have haematuria, but fewer progress to end-stage renal failure and this occurs at a later age (Jais *et al*., 2003). The autosomal recessive form (~15% of cases) involves mutations to the collagen IV $\alpha 3$ and $\alpha 4$ genes and is clinically similar to the X-linked type except that both males and females are equally affected (Lemmink *et al*., 1994; Mochizuki *et al*., 1994; Adler and Salant, 2003). Autosomal dominant disease (~5% of cases) arises from heterozygous mutations in the collagen IV $\alpha 3$ or $\alpha 4$ genes (Longo *et al*., 2002; Pescucci *et al*., 2004). Again, the clinical and pathological features are similar to those of X-linked disease except that the symptoms are less severe and renal function deteriorates slower.

Disease expression is highly variable so that at the ultrastructural level, the GBM may show several changes in contour, width and texture (Figure 1.5) (Jais *et al*., 2000, 2003). In individual cases, the majority of loops may be (i) thick and multilayered with laminations and splitting (basket weave appearance), (ii) irregular in contour with alternating thin and thick (laminated) areas or (iii) diffusely thin. GBM thickness and texture may also vary between loops so that thin, highly irregular and laminated loops may be found within the same glomerulus. In children, membrane thinning may be the most significant change, and a small number of X-linked female carriers have normal GBM (Jais *et al*., 2003; Gubler, Heidet and Antignac, 2007). Microparticles are often seen in laminated areas (Figure 1.5).

Immunolabelling has limited usefulness: occasional positivity for IgG, IgM or C3 may be seen, but the meaning of this finding is uncertain. Labelling for the collagen IV $\alpha 1$, $\alpha 3$ and $\alpha 5$ subtypes can determine the molecular makeup of the GBM and help in disease analysis. Similarly, the same panel of antibodies can be used to label epidermal basement membrane to investigate X-linked disease. For a full discussion of labelling patterns, see Hennigar and Tumlin (2009).

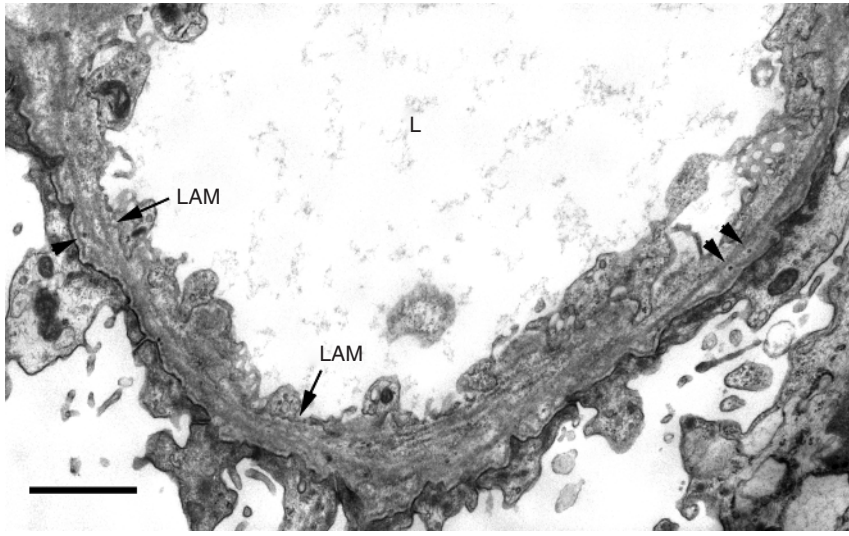

Figure 1.5 Alport's syndrome. The glomerular basement membrane shows internal laminations (LAM) and is irregular in width and contour. Microparticles (arrow heads) are seen here in laminated areas. L = capillary lumen. Bar = 1.5 μm.

1.5.2.2 Thin Basement Membrane Disease

Thin basement membrane disease (TBMD), otherwise known as benign essential haematuria or benign familial haematuria, was historically regarded as a nonprogressive renal disease with recurrent haematuria. With a greater understanding of the genetics underlying Alport's syndrome, TBMD is increasingly seen as a continuum with Alport's syndrome, and ~40% of families with TBMD have haematuria that segregates with the collagen IV α3–collagen IV α4 locus (Savige *et al.*, 2003). Indeed, misdiagnosis of Alport's syndrome as TBMD may be common, and some individuals diagnosed with TBMD are likely to be carriers of Alport's syndrome (Buzza, Wilson and Savige, 2001; Gregory, 2004; Haas, 2006).

By LM, TBMD is characterised by near-normal glomeruli with only slight mesangial expansion and proliferation; in some cases, there may be premature glomerular sclerosis. Small deposits of IgM, C3 and C1q may also be present, but these are nonspecific (Savige *et al.*, 2003). At the ultrastructural level, there is diffuse GBM thinning without splitting or lamination (Figure 1.6). Overall, the degree of thinning in TBMD cases varies. Although in some individuals there may be areas of extreme thinning (~25–30% of normal width, i.e. ~100–150 nm), overall, the

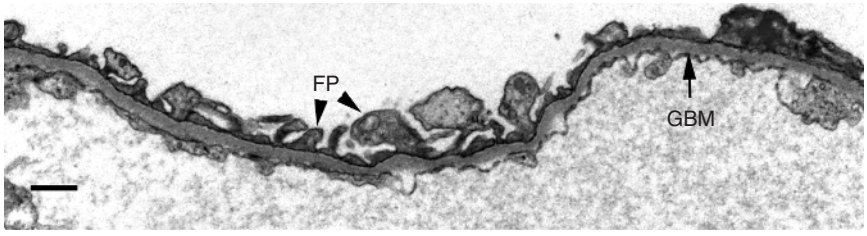

Figure 1.6 Thin basement membrane disease. The glomerular basement membrane is evenly thinned without any lamination (GBM). Here, the thinnest areas are ~90 nm in width and ~170–200 nm overall. Foot processes (FP) are essentially intact with no significant effacement. Bar = 750 nm.

GBM should be less than the normal range as established by the reporting laboratory (published values are in the range of <200–250 nm) (Savige *et al.*, 2003). Haas (2006) suggests that average GBM thickness should be less than the lower limit of the normal range (i.e. less than two standard deviations below the mean of 50 control biopsies from individuals of the same sex) and that at least 50% of individual GBM measurements should be below the lower limit of the normal range. For a diagnosis of TBMD to be made, IgA disease, minimal change, mesangiocapillary and some forms of lupus glomerulonephritis must be excluded as these may also show a degree of membrane thinning (Savige *et al.*, 2003). Note that TBMD cannot be reliably diagnosed using tissue retrieved from wax because of artefactual thinning of the GBM (Nasr *et al.*, 2007).

1.5.2.3 Diabetic Nephropathy

Approximately 40% of diabetics develop diabetic nephropathy, which is the most common cause of end-stage renal failure worldwide (Estacio and Schrier, 2001; Alsaad and Herzenberg, 2007). The principal changes that occur in both type I and type II diabetes are GBM thickening, mesangial expansion and sclerosis (Figure 1.7). Similar changes have also been reported in individuals with metabolic syndrome and glucose intolerance but no clinical manifestation of diabetes (Sanai *et al.*, 2007). Note that diabetic changes may be superimposed on those of other (concomitant) renal diseases, a situation that is increasingly common.

Based on histological appearances, diabetic nephropathy is typed as nodular, diffuse or exudative diabetic glomerulosclerosis. The nodular lesion is typified by nodules of expanded mesangial matrix containing nonspecific fibrils, collagen (including types I, III and VI), small

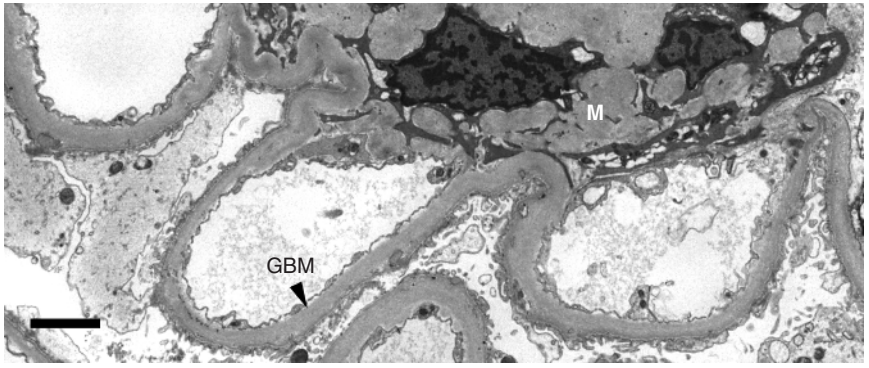

Figure 1.7 Diabetic nephropathy. Here, the glomerular basement membrane (GBM) is extensively thickened and is between ~775 and 800 nm in width. The mesangial matrix (M) shows significant expansion and consolidation. Bar = 2 um.

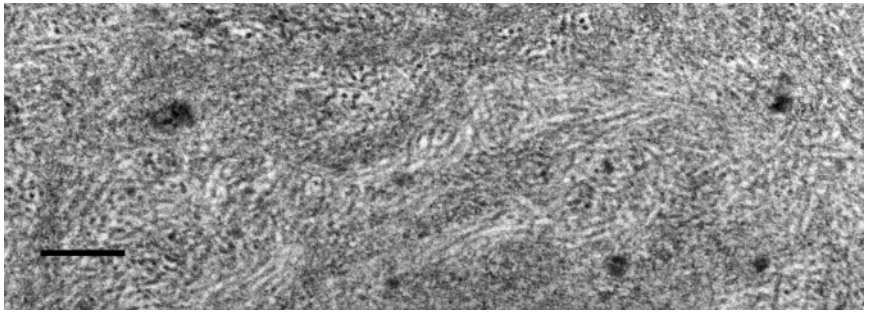

Figure 1.8 Diabetic nephropathy: Kimmelstiel–Wilson nodule. Nodules may contain ~12 nm diameter fibrils (as seen here) that may be confused with immune deposits or amyloid. Bar = 200 nm.

lipid vesicles and miscellaneous cell debris (Nishi *et al*., 2000). Kimmelstiel–Wilson nodules may contain nonspecific ~12 nm diameter fibrils (Figure 1.8) (diabetic fibrillosis) that sometimes extend into the subendothelial space and may be confused with fibrillar immune deposits (Figure 1.23) (Yasuda *et al*., 1992; Alsaad and Herzenberg, 2007). Loops are commonly displaced to the periphery of the glomerulus, and capillary lumina may contain homogeneous electron-dense material. The diffuse lesion exhibits global mesangial matrix expansion (containing some lipid and collagen fibrils) with or without mesangial hypercellularity. In contrast to the nodular type, the structure of the glomerular tufts is generally better preserved. The exudative lesion is commonly found in advanced disease. In this type, heterogeneous electron-dense

material and small lipid vesicles accumulate in the subendothelial zone to form a thickened area that encroaches on the capillary lumen (fibrin cap by LM) (Nishi *et al*., 2000). In general, GBM thickening occurs early and, as the disease progresses, may become extreme (up to four times the normal width) (Figure 1.7). Thickened GBM may also be finely laminated with occasional microparticle inclusions. Rarely, the outer GBM may show small focal areas of irregular lamination and disruption. Foot process effacement is common, and intramembranous, paramesangial and mesangial electron-dense deposits are occasionally observed. Immunolabelling may show mild to moderate linear capillary loop staining for IgG (κ and λ) and albumin (C3 negative); there may also be some nonspecific labelling for IgM and C3 in mesangium and nodules (Alsaad and Herzenberg, 2007).

1.5.2.4 Thrombotic Microangiopathy: Haemolytic Uraemic Syndrome and Thrombotic Thrombocytopaenic Purpura

Thrombotic microangiopathy (TMA) is applied to a heterogeneous group of diseases in which there is microvasculature injury with endothelial damage. Haemolytic uraemic syndrome (HUS) and thrombotic thrombocytopaenic purpura (TTP) are the two most significant forms (often with overlapping clinical features); HUS occurs as two forms, typical (classical or diarrhoea-positive HUS) and atypical (diarrhoea-negative HUS). The typical form of HUS occurs mainly in young children and accounts for 90–95% of paediatric cases. Most cases are associated with Shiga or Vero toxin-secreting *Escherichia coli* (principally strain 0157:H7), *Shigella dysenteriae* or *Streptococcus pneumoniae*. Recurrence in transplants is rare (Sánchez-Corral and Melgosa, 2010). The atypical form occurs in both adults and children, and 40–60% of patients have a mutation affecting the complement system. Thrombomodulin gene mutations have also been reported, and a few cases are related to anti–factor H autoantibodies. Recurrence in transplants is common (Sánchez-Corral and Melgosa, 2010). By contrast, TTP occurs mainly in adults and is relatively rare. Most cases are acquired; some result from acquired or congenital ADAMTS13 deficiency (George, 2009).

LM usually shows thickening of the capillary walls and a 'double contour' appearance. Fragmented red blood cells, platelets and fibrin deposition can also be found in capillary loops; there may also be

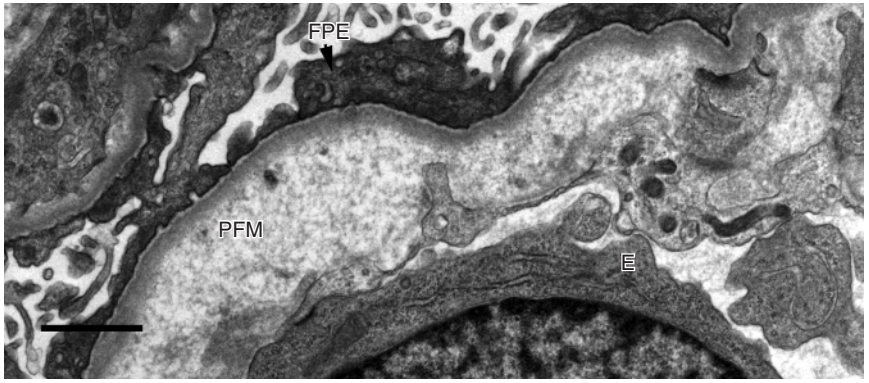

Figure 1.9 Thrombotic microangiopathy: haemolytic uraemic syndrome. The subendothelial aspect of the membrane is expanded by an accumulation of pale 'fluffy' material (PFM), and the endothelial cells (E) are swollen. Foot processes are effaced (FPE) in the area illustrated. Bar = 1 μm.

microvascular injury in arterioles (myxoid change and fibrinoid necrosis) which results in glomerular ischaemia. TEM shows swelling of the glomerular endothelium and accumulation of lucent granular, or 'fluffy', material along the subendothelial aspect of the GBM (Figure 1.9). Lucent areas can be extensive and wide and can lead to GBM reduplication. Foot processes may be partially or wholly effaced (Figure 1.9). Immunolabelling is not specific for any particular type of TMA and is commonly positive for fibrinogen (mesangium, loops and intracapillary thrombi), IgG, IgM, C3 and, rarely, IgA (loops).

1.5.3 Diseases with Granular Deposits

1.5.3.1 Membranous Glomerulonephritis

Membranous glomerulonephritis (membranous GN) is the most common cause of idiopathic nephrotic syndrome in white adults. The primary disease is autoimmune in nature; targets antigens implicated in the disease process include neutral endopeptidase, M-type phospholipase A2 receptor (PLA2R) (Beck and Salant, 2010), aldose reductase and manganese superoxide dismutase (Prunotto *et al.*, 2010). Over 75% of patients have circulating IgG4 autoantibodies to PLA2R, a podocyte transmembrane protein. Disease is initiated when antibodies bind to the PLA2R receptor on the foot processes, thereby creating subepithelial

deposits, activating the complement system and injuring the podocytes. The anti-PLA2R antibody is not found in normal individuals or those with secondary membranous GN (or other glomerular diseases), and it may therefore have a role in diagnosis and disease monitoring (Beck and Salant, 2010). Secondary disease is caused by a wide range of factors. Infectious diseases (hepatitis B, malaria, syphilis and schistosomiasis) are the most important; however, neoplasms, autoimmune diseases and a variety of drugs also play a significant role (Beck and Salant, 2010).

Membranous GN is characterised by a pattern of subepithelial and intramembranous granular electron-dense deposits with associated GBM reactions. Disease progression is staged I–IV (Ehrenreich and Churg, 1968); however, the pattern is usually mixed with multiple stages occurring together (e.g. stages II–III or III–IV). Ehrenreich and Churg (1968) define the stages as follows:

- **Stage I (early stage)**: small subepithelial deposits with no or minimal membrane reaction. Deposits may be scattered or in small clumps; some loops may have no deposits. Foot processes over deposits are effaced. The GBM may be normal or slightly uneven and irregular; it may also be thickened (depending on the amount of deposit present) (Figure 1.10).
- **Stage II (fully developed)**: numerous and extensive (sometimes contiguous) deposits that may cover entire loops. Significant membrane reaction with 'spike' formation. The GBM is irregular but only slightly and focally thickened (Figure 1.11).

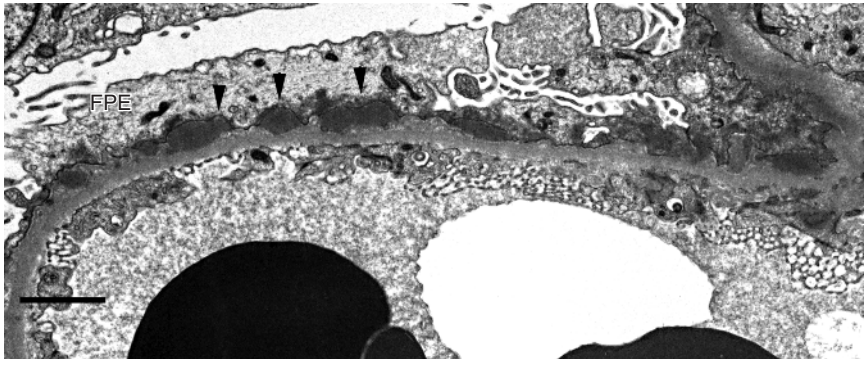

Figure 1.10 Membranous glomerulonephritis stage I (well-developed). Small to medium-sized subepithelial deposits (arrow heads) are present with minimal membrane reaction. There is foot process effacement (FPE) over deposits. Bar = 2 μm.

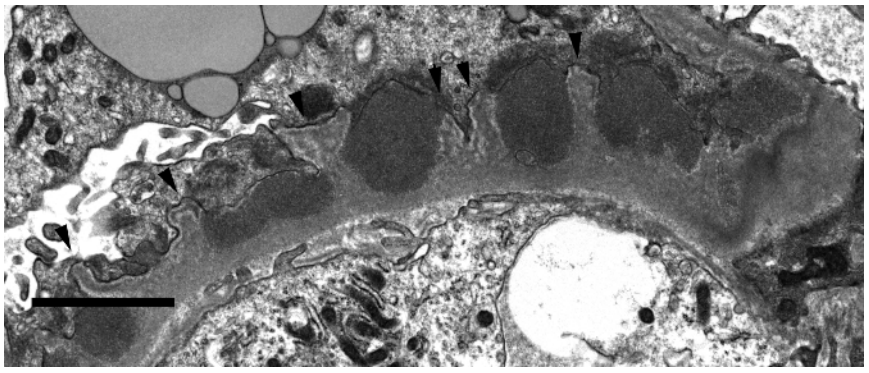

Figure 1.11 Membranous glomerulonephritis stage II. Deposits are larger, there is a significant membrane reaction to form 'spikes' (arrow heads) and there is also some membrane thickening and extensive foot process effacement. Bar = 2 μm.

- **Stage III (advanced stage)**: numerous intramembranous deposits present. Some deposits are electron dense and well demarcated, while others are pale and irregular in contour and texture (suggesting resorption). The GBM is often irregular and focally thickened (Figure 1.12).
- **Stage IV (late stage)**: intramembranous deposits lie within a significantly irregular and disorganised GBM which may be up to 10 times the normal thickness. The surface of the GBM is smooth and

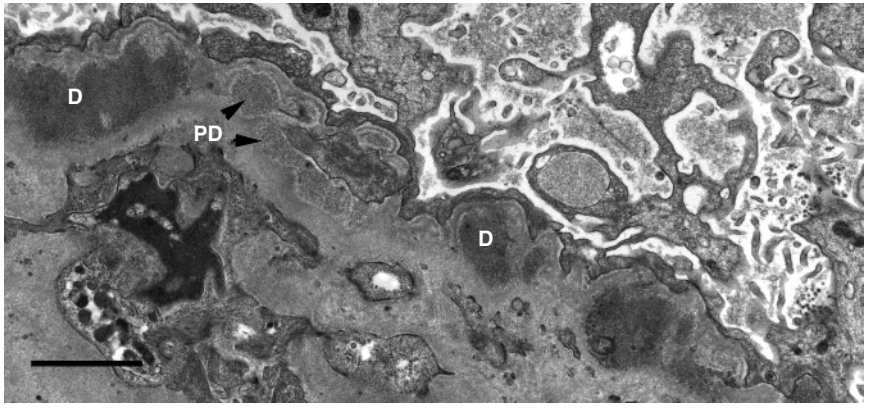

Figure 1.12 Membranous glomerulonephritis stage III. Numerous intramembranous deposits are present – seen here peripheral to mesangium. Deposits (D) vary in density; some are pale (PD) or show peripheral lucency, suggesting resorption. Bar = 2 μm.

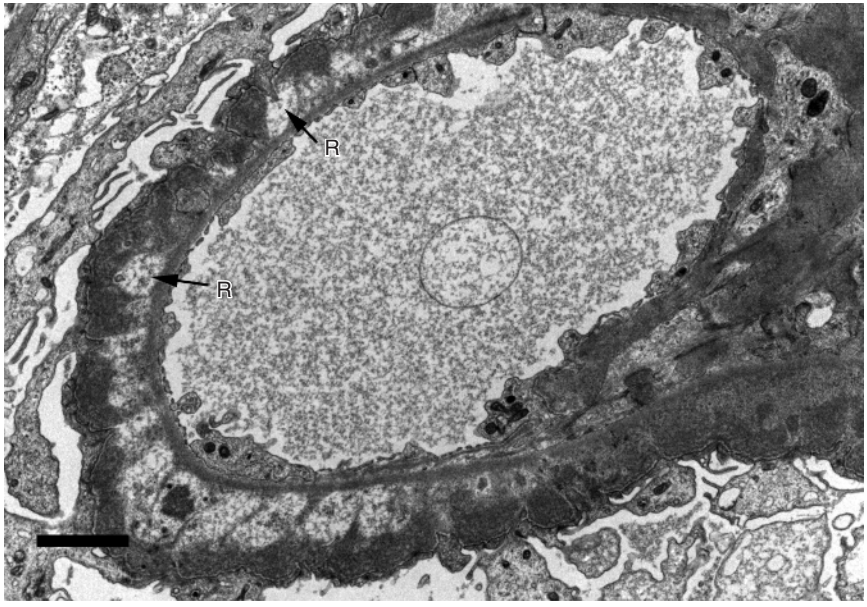

Figure 1.13 Membranous glomerulonephritis stage IV. Deposits are variable in density and texture with significant areas of resorption (R); the membrane is also highly disrupted and irregular in width and texture. Bar = 2 μm.

wavy; spikes may still be present. Deposits are highly variable in size, density and texture, suggesting varying degrees of resorption (Figure 1.13).

Ehrenreich and Churg (1968) suggest that an additional fifth, late or end stage (i.e. stage V) may be added to this classification: this final stage is characterised by capillary collapse, focal mesangial hypercellularity and sclerosis. In contrast, Coleman and Seymour (1992) include disease remission as stage V. In this system, remission is indicated by the presence of deposits that are significantly resorbed, although the GBM remains highly irregular in contour and thickness with poorly defined zones of lucency and lamination.

Finally, it is important to note that primary and secondary disease may differ in respect to both the pattern and immunological makeup of their deposits. In primary disease, the deposits are subepithelial and intramembranous, while in secondary disease there may also be mesangial and subendothelial deposition. Furthermore, the presence of TRB suggests viral infection or lupus-related disease (Beck and Salant,

2010). The finding of deposits with a fibrillar or tubular pattern suggests the presence of cryoglobulins. In respect to the immunological makeup of deposits, in primary disease there are characteristic diffuse global granular peripheral reactions to IgG (principally IgG4), often with C3 which is less intense; staining for C1q, IgM and IgA is uncommon. In secondary disease (lupus and malignancy associated), IgG2 and IgG3 are common (Beck and Salant, 2010).

1.5.3.2 Acute Post-infectious Glomerulonephritis

Acute post-infectious glomerulonephritis (PIGN) is associated with transient infection caused by numerous organisms, particularly bacteria (Rodríguez-Iturbe and Batsford, 2007). The most significant are the nephritogenic Group A β-haemolytic streptococci which cause acute post-streptococcal glomerulonephritis.

PIGN is characterised by the presence of subepithelial dome-shaped deposits (humps) around the capillary loops and mesangium (Figure 1.14). The number of deposits corresponds approximately to the level of inflammation and decreases with time. Note that humps are not specific to PIGN, and similar rounded subepithelial deposits may also occur in membranous GN (in the latter, the deposits are usually associated with a membrane reaction and are smaller and flatter than those in PIGN). Mesangial, subendothelial and intramembranous deposits may also occur, and the GBM may be disrupted because of the presence of deposits and resorbed deposits, as well as slightly irregular in width and contour. Typically, there is an endocapillary inflammatory infiltrate composed mainly of macrophages and polymorphs that may completely occlude capillary lumina; fibrin may also be present. Foot processes are commonly effaced (up to 100%), particularly over deposits (Figure 1.14). In a few cases, there is epithelial proliferation with crescent formation. Immunolabelling shows coarsely granular positivity along capillary loops for IgG and C3 and occasionally for IgM, IgA, light chains, C1q and C4. Large numbers of subepithelial deposits may create a linear or band-like effect.

Persistent infections that cause an acute diffuse proliferative glomerulonephritis with a pattern similar to that of PIGN include infectious endocarditis, bacterial infections of cerebrospinal fluid shunts (shunt nephritis), osteomyelitis and deep-seated abscess. In particular, hump-like deposits may be seen in infectious endocarditis and shunt nephritis (Rogers, Rakheja and Zhou, 2009).

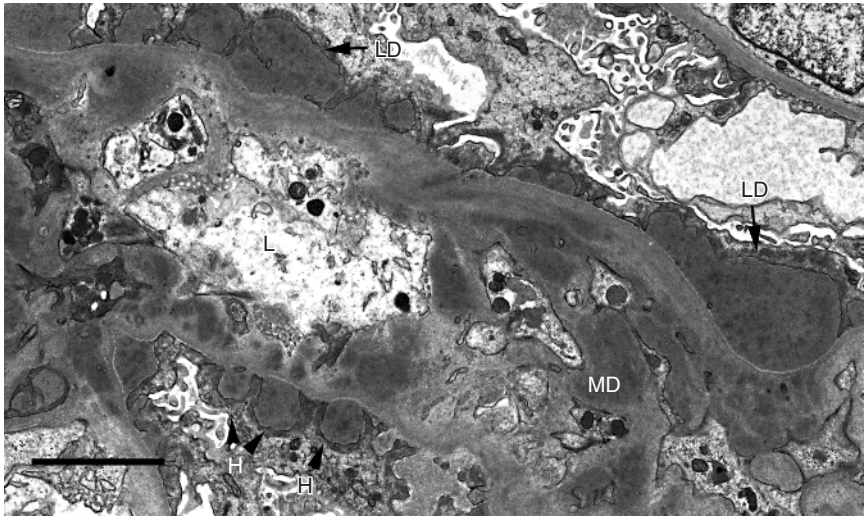

Figure 1.14 Acute post-infectious glomerulonephritis. In this case, large irregular subepithelial deposits (LD) as well as dome-shaped 'humps' (H) and mesangial deposits (MD) are present. Foot processes are effaced over the deposits. L = capillary lumen. Bar = 2.5 μm.

1.5.3.3 IgA Nephropathy (Berger's Disease) and Henoch-Schonlein Purpura Nephritis

1.5.3.3.1 IgA Nephropathy (Berger's Disease)

IgA nephropathy (IgAN) is the most common form of glomerulonephritis worldwide, and reported rates may be underestimated because of subclinical disease (McGrogan, Franssen and de Vries, 2011). The disease is heterogeneous in respect to aetiology and clinicopathological features, and its incidence varies geographically, as well as with age and ethnicity – it is also likely that the diagnosis encompasses several disease subsets (Kiryluk *et al.*, 2010). Primary disease appears to have a genetic basis. Males are affected more frequently than females (in the ratio of 6 : 1), and a significant number of IgAN patients have circulating galactose-deficient IgA1 that appears to act as an autoantigen (Kiryluk *et al.*, 2010). The mechanisms underlying the formation of IgA1 immune complexes and subsequent deposition are probably multifaceted; however, the predominant view is that the IgA1 interacts with an autoantibody (oligoclonal IgG1 and possibly IgA) to create circulating immune complexes that subsequently lodge within the mesangium

(Coppo *et al*., 2010). Secondary disease has been linked to a wide range of aetiologic agents, and the mechanism underlying the formation of deposits is unknown. There have been several systems introduced for the classification of IgAN. The most recent of these is the Oxford system, the goal of which is to identify pathological features that predict risk of progression (Cattran *et al*., 2009; Coppo *et al*., 2010). Since its introduction, the utility of the Oxford system has been validated by Herzenberg *et al*. (2011).

IgAN is characterised by mesangial IgA deposition accompanied by a variable increase in mesangial hypercellularity that is usually segmental rather than global. The mesangial matrix may also be variably increased. The GBM is sometimes thinned: this may be focal or more widespread and similar to that seen in thin basement membrane nephropathy. Deposits are often large, nodular and situated around the periphery of the mesangium; with advancing disease and mesangial enlargement, deposits may also be found within the mesangial core (Figure 1.15). Subendothelial deposits are common, but subepithelial and intramembranous deposits are rare. The presence of numerous subepithelial deposits suggests an unrelated concomitant immune-related process. IgA deposits are, in fact, found in association with a wide range of disease states (which may be classed as secondary IgAN) as well as in 4–16% of normal

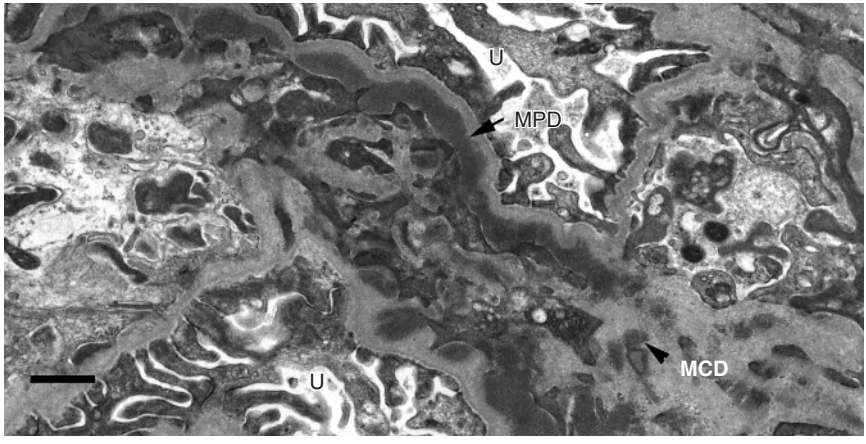

Figure 1.15 IgA nephropathy. Deposits are present within the paramesangial zone (mesangial peripheral deposits) (MPD) with some small deposits within the mesangial core proper (MCD). U = urinary space. Bar = 1 μm.

individuals (Coppo, Feehally and Glassock, 2010). Important differential diagnoses are infectious and post-infectious glomerulonephritis where the presence of IgA may mimic IgAN, and MCD where a finding of IgA may be coincidental or represent mixed disease. Additionally, significant mesangial deposits are seen in C1q nephropathy. In this disease, which may have the morphological features of MCD or FSGS, capillary wall deposits are scarce and TRBs are absent. In secondary IgAN, deposits are usually restricted to the mesangium and the mesangioproliferative process is not pronounced. Immunolabelling shows dominant or co-dominant granular diffuse mesangial IgA deposition, commonly with C3 and IgG, and sometimes with IgM. The presence of C1q suggests secondary IgAN, lupus or C1q nephropathy.

1.5.3.3.2 Henoch–Schonlein Purpura Nephritis

Henoch–Schonlein purpura nephritis (HSPN) and IgAN are related diseases sharing similar pathological and biological abnormalities. HSPN principally occurs in children (IgAN has a peak age range of 15–30 years) and is the most common vasculitis of children and young adults. In addition to the extra-renal clinical signs restricted to HSPN, the disease also has larger circulating IgA-containing complexes and a greater incidence of increased plasma IgE levels (Davin, Ten Berge and Weening, 2001).

At the ultrastructural level, HSPN is similar to IgAN except that subepithelial, intramembranous and subendothelial deposits are more common and large subepithelial deposits are frequently associated with crescents and synechiae. Mesangial deposits are principally of IgA; these commonly extend to the capillary walls. Mesangial IgG, IgM and C3 may also be present. Fibrin deposits are more frequent in HSPN than in IgAN.

1.5.3.4 Mesangiocapillary Glomerulone-phritis (Membranoproliferative Glomerulonephritis)

Primary idiopathic mesangiocapillary glomerulonephritis (MCGN) accounts for <5% of primary glomerulonephritis, and it mainly affects children and young adults. The disease is declining worldwide but is relatively common in the Middle East, South America and Africa (30–40% of cases) (Rogers, Rakheja and Zhou, 2009). MCGN is not a single entity: the term denotes a common underlying pathological mechanism and pattern of glomerular injury typified by mesangial hypercellularity with matrix expansion, structural alterations to the capillary walls (with subendothelial extension of the mesangium) and hypocomplementemia

(but with different mechanisms of complement activation). The primary forms are grouped into three types (I, II and III) based on pathological features. Secondary forms with an MCGN pattern are linked to systemic and infectious disorders and mainly occur in adults. Chronic hepatitis C infection is now known to cause a significant number of cases previously thought to be idiopathic (Alchi and Jayne, 2010). Some authorities consider type III MCGN to be a variant of type I, and some consider type II (DDD) to be distinct from MCGN based on epidemiological, morphological and aetiopathogenic criteria (Rogers, Rakheja and Zhou, 2009).

1.5.3.4.1 Type I MCGN (Classical MCGN)

Type I MCGN is defined by the deposition of immune complexes associated with the activation of the classical complement pathway (low or normal C3, low C4 and CH_{50}) – the precise identity of the putative antigen is unknown in most cases (Alchi and Jayne, 2010). Typically, there is a lobular appearance with global mesangial hypercellularity and diffuse endocapillary proliferation with infiltrating monocytes and neutrophils accompanied by an increase in mesangial matrix. Completely sclerotic mesangium may mimic diabetic-type Kimmelstiel–Wilson nodules. Deposits, which may be numerous and large, are principally subendothelial, although scattered subepithelial and mesangial deposits may also be present (Figure 1.16). Overall, the GBM becomes thickened and duplicated because of mesangial interposition ('tram-tracking' by LM) (Figure 1.16). Foot process effacement is widespread, and there may be focal microvillous transformation. Immunolabelling is strongly positive for C3 in a fine to coarse, or broad, granular pattern along capillary loops and occasionally the mesangium. There may also be labelling for IgG, IgM and, more rarely, IgA in a similar pattern; positivity for C1q, C4 and properdin may also occur.

1.5.3.4.2 Type II MCGN (Dense Deposit Disease)

Dense deposit disease (DDD) principally affects children aged 5–15 years and is associated with a serum immunoglobulin, C3 nephritic factor (C3NeF), that stabilises C3 convertase (C3bBb), thereby activating the alternative complement pathway (low C3, normal C4 and low CH_{50}) (Appel *et al.*, 2005; Alchi and Jayne, 2010). The morphological features of DDD are variable, and the glomerular hypercellularity and lobulation typical of MCGN type I are seen in only ~25% of cases. The ultrastructural appearance is distinctive and provides a definitive diagnosis.

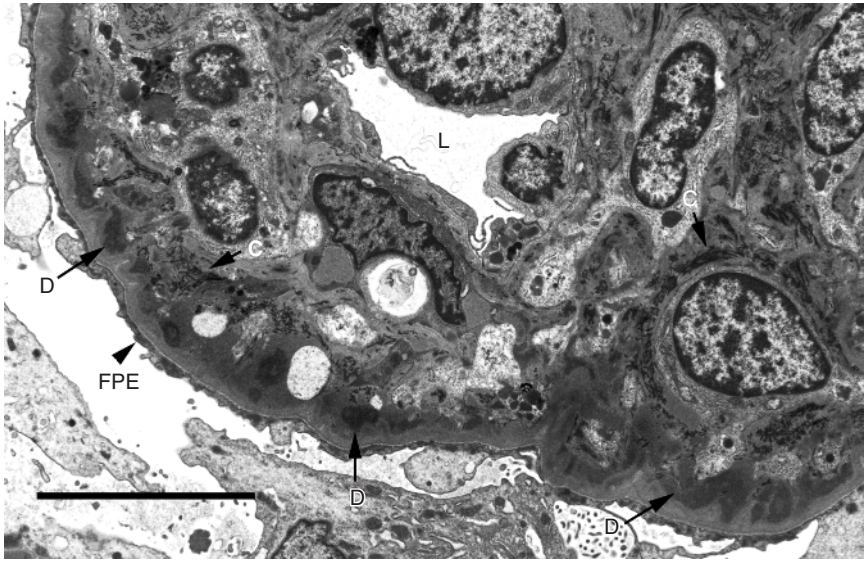

Figure 1.16 Mesangiocapillary glomerulonephritis type I. Large heterogeneous deposits (D) are seen around the inner aspect of the capillary loop and the paramesangial zone. These deposits were originally subendothelial in location but have been incorporated into the capillary wall, which is significantly thickened because of mesangial cell interposition and matrix formation. Fibrillar collagen (C) is also seen within the thickened wall and mesangium. There are no subepithelial deposits present in this example, but foot processes are totally effaced (FPE). L = capillary lumen. Bar = 7.5 μm.

Capillary loops have continuous electron-dense homogeneous deposits along the subendothelial aspect of the GBM; these may be within the inner portion of the membrane or across its entire width (Figure 1.17). The effect is a band or ribbon-like appearance that is often referred to as a linear 'transformation', although occasionally the deposits may be interrupted, in which case they have the appearance of a string of sausages (sometimes called bacon rash deposits) (Alchi and Jayne, 2010). Deposits may also be found in the paramesangium, mesangium, Bowman's capsule, tubular basement membranes and blood vessel walls. Subepithelial and subendothelial deposits may be found in cases with the LM features of acute proliferative glomerulonephritis and membranous glomerulopathy. Mesangial interposition and hypercellularity may also be present. Immunolabelling shows intense linear capillary loop and

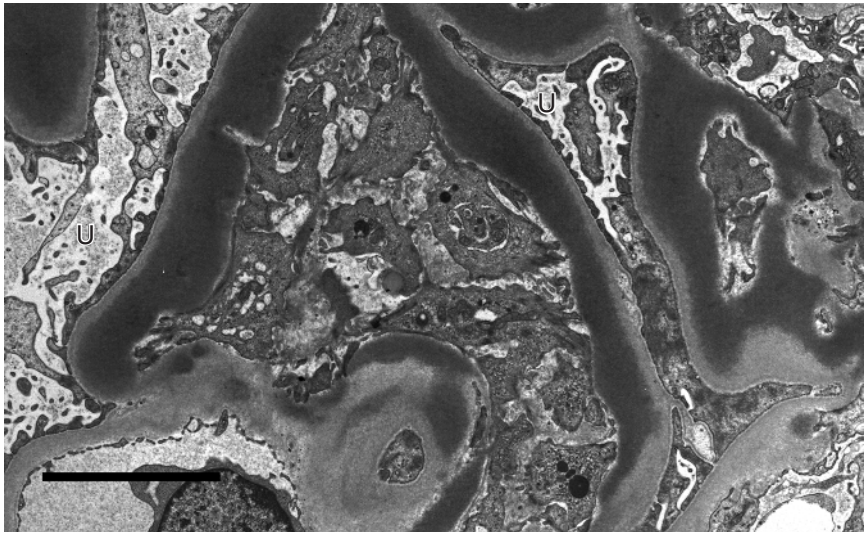

Figure 1.17 Mesangiocapillary glomerulonephritis type II (dense deposit disease). A typical continuous linear electron-dense homogeneous deposit is seen around the inner aspect of the capillary basement membrane (the feature in the centre of the image may be an occluded loop or mesangium). U = urinary space. Bar = 5 μm.

mesangial positivity for C3, generally without C1q and C4. Deposits are not typical immune complexes, so immunoglobulins are therefore generally absent, although IgM, IgG and IgA have been reported (Alchi and Jayne, 2010).

1.5.3.4.3 Type III MCGN

In type III MCGN, both the alternative and terminal complement pathways are activated (low C3, normal C4 and low C5–C9) (Alchi and Jayne, 2010).

The gross features of MCGN types I and III are similar but, although mesangial hypercellularity may be less, there is often a more lobular appearance and GBM thickening is more pronounced with significant tram tracking. Two types of type III MCGN are recognised, that of Burkholder, Marchand and Krueger (1970) and that of Strife *et al.* (1977) and Anders *et al.* (1977). The characteristic features of these subtypes are large subepithelial deposits with a membrane reaction similar to 'spikes' (type III of Burkholder), and subendothelial and

intramembranous deposits that span the width of the GBM (from the subendothelial to the subepithelial zone) with associated membrane disruption and lamination (type III of Strife and Anders). Immunolabelling reveals coarse granular staining for C3 along capillary loops and in mesangium in ~50% of cases. In the other 50%, the C3 labelling is combined with staining for IgG with lesser and more variable reactions for IgM and/or IgA.

1.5.3.5 Systemic Lupus Erythematosus

Systemic lupus erythematosus (SLE) is a complex autoimmune disease with a wide range of clinical presentations. SLE causes inflammation in multiple organ systems, particularly the kidney, skin, serosal membranes, central nervous system and joints. Approximately 15–55% of individuals with SLE develop lupus nephritis (Siso *et al*., 2010). SLE occurs at all ages and in both sexes (with a female-to-male ratio of ~10:1), but it particularly affects premenopausal women with a predilection for those of Asian and African American descent. Lupus nephritis is generally more severe in children, males and patients of Asian, Hispanic and African descent (Venuturupalli and Wallace, 2007; Stokes, Nasr and D'Agati, 2009). Some cases of SLE are idiopathic, but the disease may be precipitated or aggravated by numerous agents including drugs, viral infection (particularly HIV), ultraviolet light and hormones – there may also be genetic factors involved (Stokes, Nasr and D'Agati, 2009). A wide variety of circulating autoantibodies have been found in SLE; the profile of these antibodies persists despite the level of disease activity and state of remission (Fattal *et al*., 2010). Levels of immunoglobulins (IgG) directed against single- and double-stranded DNA (antinuclear antibodies), Epstein–Barr virus and hyaluronic acid all increase; however, some specific IgM levels decrease, and this profile is highly specific (>88%) for SLE (Fattal *et al*., 2010). Antibodies against double-stranded DNA predominate in glomerular immune deposits. The site of immune complex deposition within the glomerulus may be determined by the type, specificity and physicochemical characteristics of the immunoglobulins involved and the circulating immune complex load (Stokes, Nasr and D'Agati, 2009).

To improve diagnosis and the interpretation of the renal pathology associated with SLE, several classification systems have been developed. The current system is the International Society of Nephrology/Renal Pathology Society (ISN/RPS) 2003 classification of lupus nephritis, which is based on previous World Health Organisation classification

systems (Weening *et al*., 2004; D'Agati, 2007). The ISN/RPS classification is based on an integrated analysis of the LM and immunolabelling findings and, while TEM is not required for classification, it is highly recommended.

The range of TEM findings in SLE is summarised in Table 1.2. Most cases have finely granular, medium-density mesangial deposits, usually in combination with subepithelial and/or subendothelial deposits; organised deposits also occur (Figures 1.18 and 1.19). Organised material may consist of fingerprint deposits (Figure 1.20) or lattice-like, fibrillar or tubular deposits, the latter sometimes organised in parallel arrays. Organised deposits may be associated with circulating type III mixed cryoglobulin (Stokes, Nasr and D'Agati, 2009). Some cases of SLE also have large numbers of TRBs in capillary endothelial cells (Figure 1.18), although numbers vary and only a few may be present, particularly during treatment. Characteristically, immunolabelling is positive for IgG (generally the strongest), IgA, IgM, C3 and C1q ('full-house' labelling). Nuclei may show staining for IgG because of the presence of circulating antinuclear antibodies.

1.5.3.6 Monoclonal Immunoglobulin Deposition Disease

Monoclonal immunoglobulin deposition disease (MIDD) is a rare systemic disease that involves the deposition of monoclonal immunoglobulins in several organs, with most patients having kidney involvement. Three types of MIDD have been described: light-chain deposition disease (LCDD), heavy-chain deposition disease (HCDD) and mixed light- and heavy-chain deposition disease (LHCDD) (Lin *et al*., 2001; Basnayake *et al*., 2011). LCDD and HCDD appear to be similar clinically; LCDD is the most common type, and only a few LHCDD and HCDD cases have been reported.

Morphologically, LCDD and HCDD are similar. Early cases may show little change but, as the disease progresses, mesangial proliferation is followed by a membranoproliferative pattern. Finally, the characteristic appearance is that of nodular sclerosis. Immunolabelling shows a characteristic linear pattern of positivity along the basement membranes of glomerular capillaries and tubules. In LCDD, monoclonal κ or λ light chains may be present, while in HCDD, α heavy chains predominate with a small number of cases involving γ or u heavy chains. (Gokden, Barlogie and Liapis, 2008; Basnayake *et al*., 2011). By TEM, deposits are finely granular or powdery in appearance and can usually be found in the

Table 1.2 Abbreviated ISN/RPS 2003 classification of SLE: immunolabelling and TEM features (based on Weening *et al*., 2004; Stokes, Nasr and D'Agati, 2009).

Class I: minimal mesangial lupus nephropathy

No change by LM. Mesangial immune deposits by immunolabelling and TEM. Minimal foot process effacement.

Class II: mesangial proliferative lupus nephropathy

Mesangial hypercellularity. Mesangial deposits with rare isolated and small subepithelial or subendothelial deposits involving the capillary walls in some cases (but not visible by LM). The presence of subendothelial deposits visible by LM warrants designation as class III/IV depending on the percentage of glomeruli affected.

Class III: focal lupus nephropathy (involving less than 50% of glomeruli)

(A) active lesions; (A/C) active and chronic lesions; (C) chronic lesions

Focal disease: in assessing the extent of the lesions, both active and sclerotic lesions must be included. Focal or diffuse mesangial alterations, including proliferation and deposits. Subendothelial deposits are also present; usually segmental. Small subepithelial deposits may be present; if these affect >50% of glomerular surface area in a minimum of 50% of glomeruli (by LM or IF), an additional (combined) diagnosis of membranous lupus nephritis (class V) may be given.

Class IV: diffuse lupus nephropathy (involving 50% or more of glomeruli)

Diffuse segmental (IV-S) or global (IV-G)

(A) active lesions; (A/C) active and chronic lesions; (C) chronic lesions

Typically shows diffuse subendothelial deposits, with or without mesangial alterations. Scattered subepithelial deposits are often found in class IV disease: a combined diagnosis of IV/V is if these deposits involve at least 50% of the surface of capillary loops in a minimum of 50% of glomeruli by LM or immunolabelling.

IV-S: segmental endocapillary proliferation encroaching on capillary lumina ± necrosis

IV-G: diffuse and global endocapillary, extracapillary or mesangiocapillary proliferation or widespread wire loops. Includes cases with extensive (diffuse and global) subendothelial deposits with little or no proliferation.

Class V: membranous lupus nephropathy

Membranous disease with global or segmental continuous granular subepithelial immune deposits (with membrane thickening and spikes in established disease), often combined with mesangial deposits ± mesangial hypercellularity. Scattered subendothelial deposits by TEM or immunolabelling. However, if deposits are present by LM, then a combined diagnosis of class III/V or class IV/V is warranted, depending on their distribution.

Class VI: advanced sclerosing lupus nephropathy (≥90% sclerosed glomeruli without residual activity)

Biopsies showing ≥90% global glomerulosclerosis with clinical or pathological evidence that the sclerosis is caused by lupus nephritis, but with no evidence of ongoing active glomerular disease. Residual deposits in sclerosing glomeruli. May represent the advanced stage of chronic class III, IV or V disease.

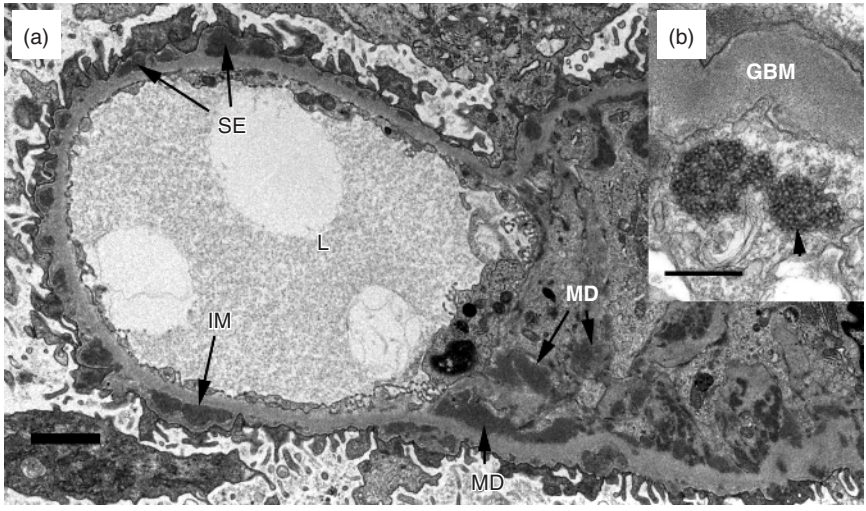

Figure 1.18 Systemic lupus erythematosus. (a) In addition to mesangial and paramesangial deposits (MD), subepithelial (SE) and intramembranous deposits (IM) are present around the capillary loop. There is only minor effacement of capillary loops. L = capillary lumen. Bar = 2 µm. (b, inset) A tubuloreticular body (arrow head) in an endothelial cell: these are sometimes found in large numbers in SLE. GBM = glomerular basement membrane. Bar = 500 nm.

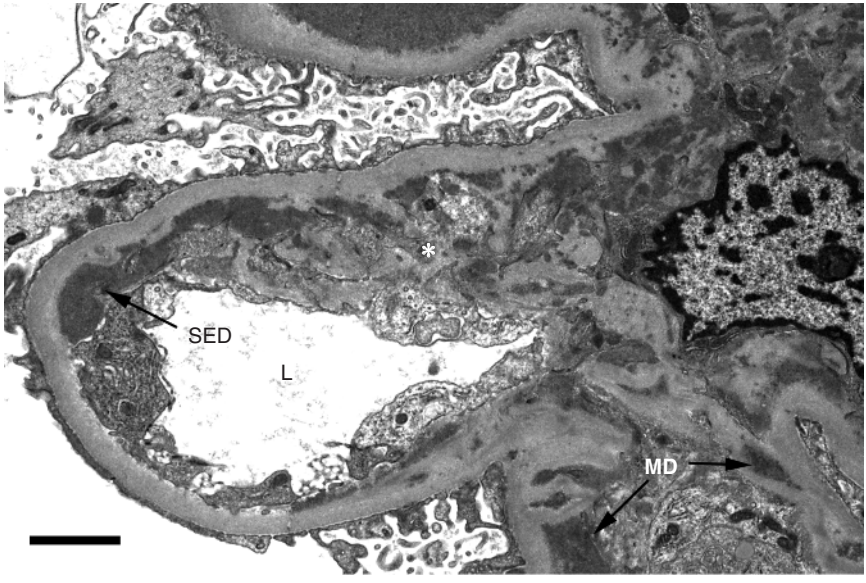

Figure 1.19 Systemic lupus erythematosus. In addition to mesangial and paramesangial deposits (MD), there are extensive subendothelial deposits (SED) with endothelial cell swelling and possible mesangial interposition (*). In addition, the GBM appears to be slightly thickened and there is some foot process effacement. L = capillary lumen. Bar = 2 µm.

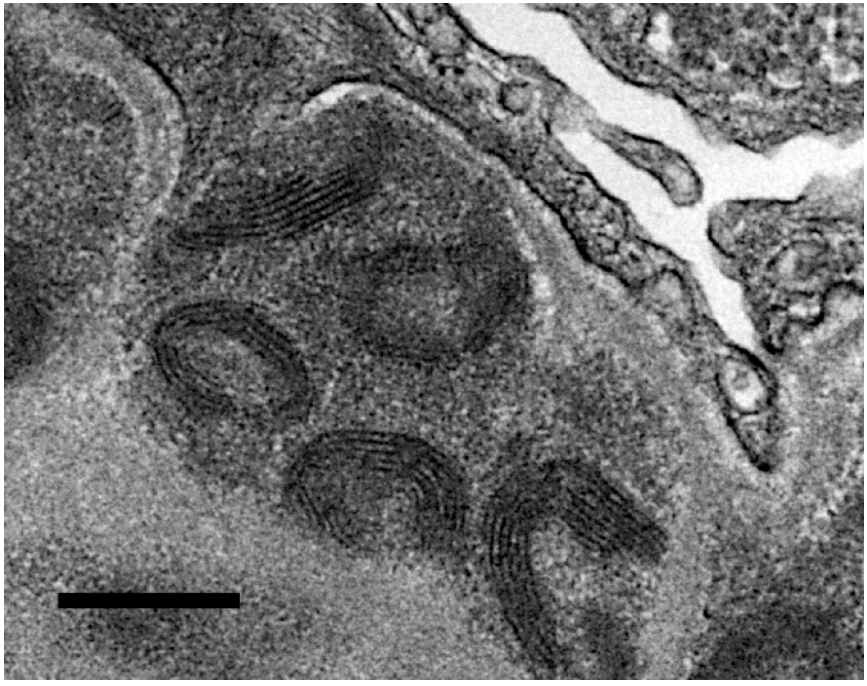

Figure 1.20 Systemic lupus erythematosus – organised deposit. Organised deposits with a whorl or 'fingerprint' arrangement of this type are sometimes seen in cases of SLE.

mesangium and along the GBM, tubular basement membranes and Bowman's capsule. In the glomerulus, linear deposition usually occurs along the lamina rara interna of the GBM and sometimes within the lamina densa (Figure 1.21), a pattern that may mimic Type II MCGN (DDD) (Figure 1.17). In tubules, deposition is between the basement membrane and the interstitium. Sometimes, deposition is not widespread and careful searching is required (Gokden, Barlogie and Liapis, 2008). LCDD commonly recurs in transplants (Leung *et al.*, 2004).

1.5.4 Diseases with Organised Deposits

1.5.4.1 Amyloidosis

Deposition of amyloid can occur in many organs, and at least 25 types of amyloid have been identified, all with different precursor proteins. All amyloid deposits have been found to contain up to 15% of amyloid P, a nonfibrillary glycoprotein identical to serum amyloid P (Vowles,

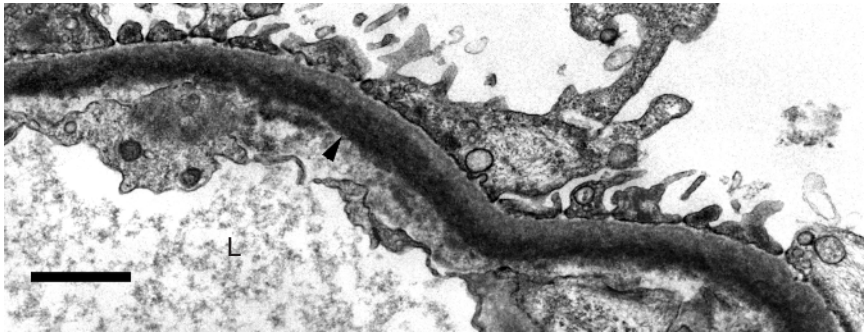

Figure 1.21 Light-chain deposition disease (κ light-chain disease). κ light chains are seen as a powdery linear deposit (arrow head) that may be regarded as either intramembranous (within the lamina densa) or within the lamina rara interna of the GBM. There is also minor foot process effacement. L = capillary lumen. Bar = 1 μm.

2008). Many amyloid types may be found in the kidney, most commonly AL amyloid (derived from immunoglobulin light chains; primary and myeloma-associated amyloidosis), and more rarely AA (derived from serum amyloid A; reactive secondary amyloidosis) and AH (derived from immunoglobulin heavy chains; primary and myeloma-associated amyloidosis).

Amyloid may infiltrate all areas of the glomerulus, including the mesangium, the GBM, Bowman's capsule and the urinary space. By LM, amyloid deposition appears as amorphous hyaline material which is Congo red positive (Table 1.1). However, note that small deposits may be missed by LM, and TEM examination is critical. At the ultrastructural level, amyloid deposits consist of randomly arranged, long, straight, nonbranching fibrils ~7–12 nm in width (Table 1.1, Figure 1.22). Fibrils may sometimes appear to penetrate cell membranes (Figure 1.22). More organised fibrils may be seen as expanding, almost parallel arrays (cascades) (Figure 1.22); this spiculated type of amyloid deposition can mimic the appearance of GBM 'spikes' with silver staining. TEM does not differentiate the various amyloid types. Immunolabelling may show monotypic light-chain staining in some cases of AL-associated amyloidosis; labelling for immunoglobulins, complement components, fibrinogen and albumin is negative.

1.5.4.2 Fibrillary Glomerulonephritis

Fibrillary glomerulonephritis (fibrillary GN) is rare, predominantly affects Caucasians and has a peak incidence in the fifth to sixth decades of

Figure 1.22 Amyloid. Fibrils with a random organisation (R) and in parallel arrays (P) are seen in this image, the latter appearing to penetrate (or cascade or flow from) the overlying epithelial cell (E). Bar = 750 nm.

life; it is associated with a wide range of conditions that result in chronic immune stimulation, including systemic disorders and viral infections such as HIV (Haas *et al*., 2000). Association with a lymphoproliferative disorder is uncommon (<5% of cases). The disease can recur in renal transplants (Herrera and Turbat-Herrera, 2010).

LM can show many changes including mesangial expansion and proliferation, capillary wall thickening (segmental or diffuse), segmental collapse and crescents. TEM is definitive with the finding of fibrillar deposits in the mesangium and capillary walls (subepithelial, subendothelial and transmembrane) (Figure 1.23). Fibrils are ~13-29 nm in diameter and must be distinguished from amyloid and nonspecific fibrillar deposits using a combination of TEM, LM and immunolabelling criteria (Table 1.1). Characteristically, mesangial and/or peripheral capillary walls show linear or pseudo-linear positivity for IgG (mostly IgG4), C3 and κ and λ light chains (Herrera and Turbat-Herrera, 2010). Amyloid-P component may co-localise with the fibrils.

1.5.4.3 Immunotactoid Glomerulonephritis

Immunotactoid glomerulonephritis (immunotactoid GN) is less common than fibrillary GN (~100 times rarer), predominantly affects Caucasians and has a peak incidence after 60 years of age. Importantly, immunotactoid GN is normally associated with lymphoproliferative disorders and,

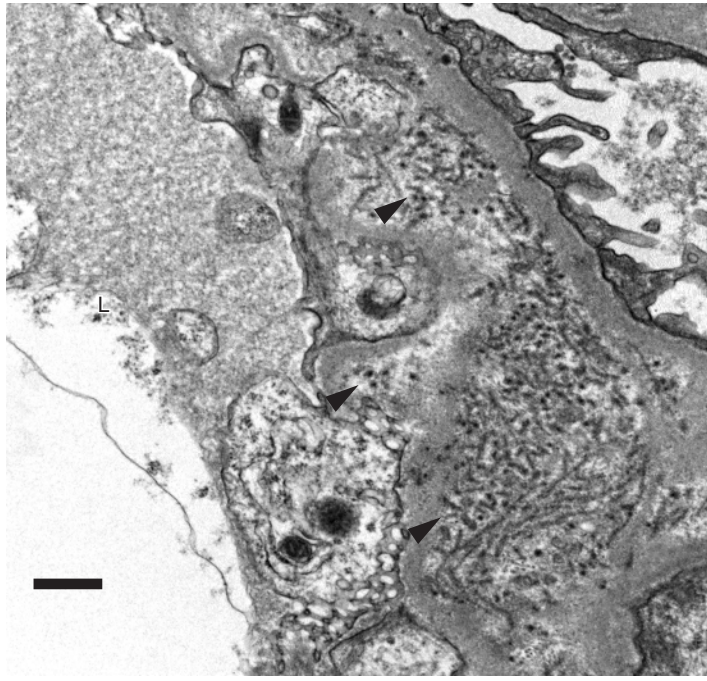

Figure 1.23 Fibrillary glomerulonephritis. Immune fibrils (arrow heads) ~12–18 nm in diameter are seen in the capillary basement membrane. L = capillary lumen. Bar = 500 nm.

more rarely, viral infection (Markowitz *et al*., 1998; Haas *et al*., 2000; Herrera and Turbat-Herrera, 2010). Like fibrillary GN, immunotactoid GN recurs in transplants (Herrera and Turbat-Herrera, 2010).

The LM appearance is variable and nonspecific, so TEM is required for diagnosis. Ultrastructurally the deposits are seen as extracellular, long, nonbranching tubules (Figure 1.24), sometimes with a lattice-like pattern; tubules may be similar to those seen in cryoglobulinaemia (Figure 1.25) (Ivanyi and Degrell, 2004). Tubules are usually densely packed in parallel arrays, but are sometimes random. Overall tubule diameter ranges from 10 to 90 nm but is usually >30 nm (Table 1.1, Figure 1.24). The tubules may be embedded in an amorphous or granular material or within the background matrix. All cases generally show mesangial deposits, but the capillary loops can also be involved. Immunolabelling commonly shows patchy granular or pseudolinear

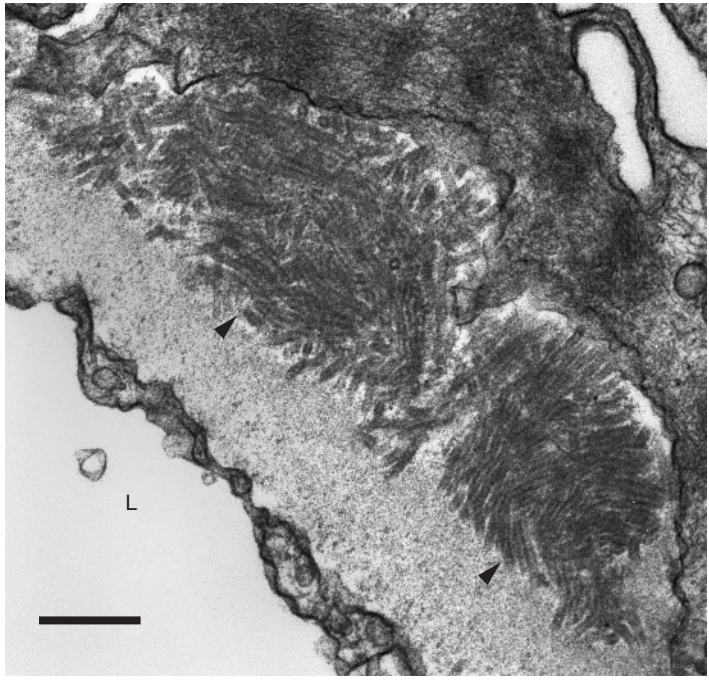

Figure 1.24 Immunotactoid glomerulonephritis. Immune deposits organised as densely packed and randomly organised hollow tubules (arrow heads) ~35 nm in diameter are seen here in a subepithelial location. L = capillary lumen. Bar = 350 nm.

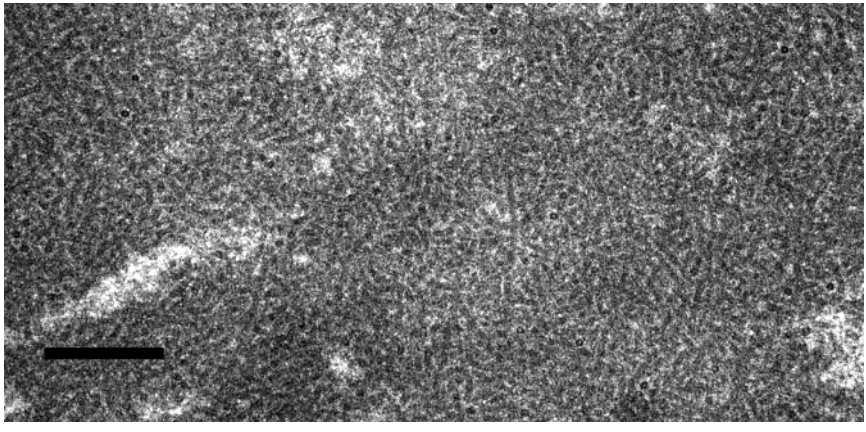

Figure 1.25 Cryoglobulinaemic glomerulonephritis. The appearance of cryoglobulin deposits varies considerably. In this case, the deposits are seen as randomly organised straight or slightly curved tubules ~30 nm in diameter. The tubules are set in a finely granular amorphous background and are not quite as distinctly formed as the tubules seen in immunotactoid. Bar = 500 nm.

positivity for IgG and C3 (peripheral and mesangial), and there may be light-chain restriction (κ more than λ). Labelling for IgM, IgA and C1q is uncommon (Herrera and Turbat-Herrera, 2010).

1.5.4.4 Cryoglobulinaemic Glomerulonephritis

Cryoglobulins are mixtures of rheumatoid factor, immunoglobulins and hepatitis C virus RNA that undergo reversible precipitation below 37 °C. Three types have been identified: type I, which contains monoclonal immunoglobulins only (usually IgM); type II, a mixture of monoclonal immunoglobulins (usually IgM) and polyclonal IgG and type III, a mixture of polyclonal immunoglobulins (usually IgM) and polyclonal IgG. Types II and III contain rheumatoid factor; type I does not. 'Mixed' cryoglobulinaemia represents a mixture of types II and III, with Hepatitis C being responsible for >90% of such cases (mainly type II, with a small number of type III) (Charles and Dustin, 2009). Additional cases are principally caused by infectious agents (mainly viral), autoimmune diseases and neoplasms; this leaves ~5% of cases in which no cause is identified, and these are termed essential (Charles and Dustin, 2009; Matignon *et al*., 2009). Approximately 20% of individuals with cryoglobulinaemia develop renal disease.

In cryoglobulinaemic glomerulonephritis, the pattern of glomerular changes is diverse and ranges from mild mesangial hypercellularity through to proliferative disease with an MCGN type I pattern. Immunolabelling depends on the cryoglobulin involved. Deposits may be found in any part of the glomerulus, but particularly in the subendothelial region, mesangium and thrombi. Thrombi often show the most characteristic ultrastructural features. Overall, the appearance varies considerably from coarsely granular to fibrillar or tubular (with a random orientation) (Figure 1.25), depending on the cryoglobulins involved and the orientation of the material within the section. Classical granular immune deposits may also be present. Typically, deposits of mixed cryoglobulins are described as consisting of paired, curved microtubular or annular structures (with spokes) ~25–40 nm in diameter. Monoclonal cryoglobulins are described as fibrils (seen singly or in bundles, and sometimes with cross-hatching) or tubules with a fingerprint organisation.

1.5.5 Hereditary Metabolic Storage Disorders

A number of rare hereditary storage diseases cause renal complications. Here we include only Fabry's disease and lecithin cholesterol acyltransferase (LCAT) deficiency as illustrative examples.

1.5.5.1 Fabry's Disease

Fabry's disease is an X-linked lysosomal storage disorder that affects both sexes. The incidence is ~1:40 000–1 : 117 000 (Torra, 2008). Affected individuals have no, or significantly reduced, α-galactosidase A activity that results in the lysosomal accumulation of glycosphingolipids, mainly globotriaosylceramide (GL-3). Nephropathy develops by age ~27 years followed by end-stage renal disease and death, generally by the age of 60. Enzyme replacement therapy can stabilise glomerular filtration in early cases (Öqvist *et al*., 2009).

By LM, most podocytes have a vacuolated (or honeycomb) appearance, or may contain myelin-like inclusions. Unlike LCAT deficiency, the mesangial and endothelial cells may not be affected. At the ultrastructural level, podocytes are seen to contain large numbers of abnormal secondary lysosomes with a lamellar or myelin-like appearance (zebra bodies) (Figure 1.26) (Torra, 2008). The lamellae may be loosely arranged. Lysosomal deposits similar to those seen in Fabry's disease have also been reported in silicosis, and as the result of various drug

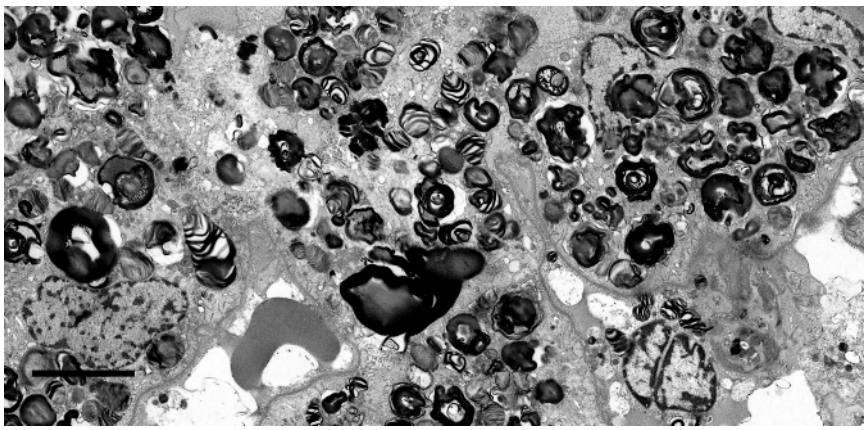

Figure 1.26 Fabry's disease. Podocytes contain large abnormal secondary lysosomes that are either solid or lamellar (myelin-like) in appearance. Bar = 5 μm.

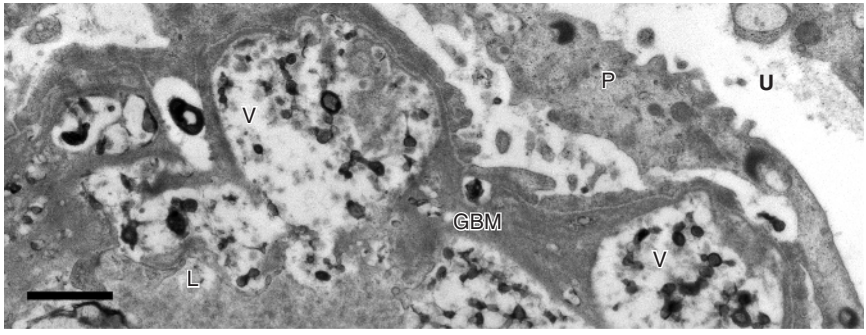

Figure 1.27 Lecithin cholesterol acyltransferase deficiency. Electron-lucent vesicles (V) with electron-dense cores of various types are seen within the glomerular basement membrane (GBM). L = capillary lumen; U = urinary space and P = podocyte. Bar = 1.5 μm.

treatments (amiodarone, chloroquine and hydroxychloroquine) (Öqvist *et al*., 2009). Immunolabelling is negative.

1.5.5.2 Lecithin Cholesterol Acyltransferase Deficiency

LCAT deficiency is a very rare hereditary autosomal recessive disorder currently described in ~50 families world-wide. Patients in their third and fourth decades usually develop renal failure, with glomerulosclerosis being a major cause of morbidity and mortality (Miarka *et al*., 2011).

By LM, glomeruli have a honeycomb appearance in all compartments because of the extraction of lipid deposits during processing. At the ultrastructural level, heterogeneous lipid deposits are seen in the GBM (subepithelial, intramembranous and subendothelial locations); these have the appearance of electron-lucent vacuoles with a dense core consisting of curvilinear fibrils or lamellae (Figure 1.27). Mesangial deposits appear as large lucent areas with irregular dense cores. Immunolabelling is usually negative or nonspecific, but silver stains can show spikes in the GBM, mimicking membranous GN.

REFERENCES

Abrahamson, D.R., Hudson, B.G., Stroganova, L. *et al*. (2009) Cellular origins of type IV collagen networks in developing glomeruli. *Journal of the American Society of Nephrology*, **20**, 1471–1479.

Adler, S.G. and Salant, D.J. (2003) An outline of essential topics in glomerular pathophysiology, diagnosis, and treatment for nephrology trainees. *American Journal of Kidney Diseases*, **42** (2), 395–418.

Alchi, B. and Jayne, D. (2010) Membranoproliferative glomerulonephritis. *Pediatric Nephrology*, **25**, 1409–1418.

Alsaad, K.O. and Herzenberg, A.M. (2007) Distinguishing diabetic nephropathy from other causes of glomerulosclerosis: an update. *Journal of Clinical Pathology*, **60**, 18–26.

Anders, D., Agricola, B., Sippel, M. and Thoenes, W. (1977) Basement membrane changes in membranoproliferative glomerulonephritis. II. Characterisation of a third type by silver impregnation of ultra thin sections. *Virchow Archives A: Pathological Anatomy and Histology*, **376** (1), 1–19.

Appel, G.B., Cook, H.T., Hageman, G. *et al.* (2005) Membranoproliferative glomerulonephritis type II (dense deposit disease): an update. *Journal of the American Society of Nephrology*, **16**, 1392–1404.

Barker, D.F., Hostikka, S.L., Zhou, J. *et al.* (1990) Identification of mutations in the COL4A5 collagen gene in Alport syndrome. *Science*, **248** (4960), 1224–1227.

Basnayake, K., Stringer, S.J., Hutchison, C.A. and Cockwell, P. (2011) The biology of immunoglobulin free light chains and kidney injury. *Kidney International*, **79**, 1289–1301.

Beck, J.H. and Salant, D.J. Jr (2010) Membranous nephropathy: recent travels and new roads ahead. *Kidney International*, **77**, 765–770.

Bonsib, S.M. (2007) Renal anatomy and histology, in *Heptinstall's Pathology of the Kidney*, vol. 1, 6th edn (eds J.C. Jennette, J.L. Olson, M.M. Schwartz and F.G. Silva), Lippincott Williams and Wilkins, Philadelphia, PA, pp. 1–70.

Burkholder, P.M., Marchand, A. and Krueger, R.P. (1970) Mixed membranous and proliferative glomerulonephritis: a correlative light, immunofluorescence, and electron microscopic study. *Laboratory Investigation*, **23** (5), 459–479.

Butkowski, R.J., Wieslander, J., Kleppel, M. *et al.* (1989) Basement membrane collagen in the kidney: regional localization of novel chains related to collagen IV. *Kidney International*, **35**, 1195–1202.

Buzza, M., Wilson, D. and Savige, J. (2001) Segregation of hematuria in thin basement membrane disease with haplotypes at the loci for Alport syndrome. *Kidney International*, **59**, 1670–1676.

Cattran, D.C., Coppo, R., Cook, H.T. *et al.* (2009) The Oxford classification of IgA nephropathy: rationale, clinicopathological correlations, and classification. *Kidney International*, **76**, 534–545.

Charles, E.D. and Dustin, L.B. (2009) Hepatitis C virus-induced cryoglobulinemia. *Kidney International*, **76**, 818–824.

Coleman, M., Haynes, W.D.G., Dimopoulos, P. *et al.* (1986) Glomerular basement membrane abnormalities associated with apparently idiopathic hematuria: ultrastructural morphometric analysis. *Human Pathology*, **17**, 1022–1030.

Coleman, M. and Seymour, A.E. (1992) The kidney, in *Diagnostic Ultrastructure of Non-neoplastic Diseases* (eds J.M. Papadamitiou, D.W. Henderson and D.V. Spagnolo), Churchill Livingstone, Edinburgh, pp. 374–416.

Coleman, M. and Stirling, J.W. (1991) Glomerular basement membrane thinning is acquired in minimal change disease. *American Journal of Nephrology*, **11**, 437–438.

Coppo, R., Feehally, J. and Glassock, R.J. (2010) IgA nephropathy at two score and one. *Kidney International*, **77**, 181–186.

Coppo, R., Troyanov, S., Camilla, R. *et al.* (2010) The Oxford IgA nephropathy clinicopathological classification is valid for children as well as adults. *Kidney International*, **77**, 921–927.

D'Agati, V.D. (2007) Renal disease in systemic lupus erythematosus, mixed connective tissue disease, Sjögren's syndrome, and rheumatoid arthritis, in *Heptinstall's Pathology of the Kidney*, vol. 1, 6th edn (eds J.C. Jennette, J.L. Olson, M.M. Schwartz and F.G. Silva), Lippincott Williams and Wilkins, Philadelphia, PA, pp. 518–612.

D'Agati, V.D. (2008) Podocyte injury in focal segmental glomerulosclerosis: lesson from animal models (a play in five acts). *Kidney International*, **73**, 399–406.

D'Agati, V.D., Fogo, A.B., Bruijn, J.A. and Jennette, J.C. (2004) Pathologic classification of focal segmental glomerulosclerosis: a working proposal. *American Journal of Kidney Disease*, **43** (2), 368–382.

Davin, J-C., Ten Berge, I.J. and Weening, J.J. (2001) What is the difference between IgA nephropathy and Henoch–Schönlein purpura nephritis? *Kidney International*, **59**, 823–834.

Dember, L.M. (2006) Amyloidosis-associated kidney disease. *Journal of the American Society of Nephrology*, **17**, 3458–3471.

Dische, F.E. (1992) Measurement of glomerular basement membrane thickness and its application to the diagnosis of thin-membrane nephropathy. *Archives of Pathology and Laboratory Medicine*, **116** (1), 43–49.

Edwards, K., Griffiths, D., Morgan, J. *et al.* (2009) Can the choice of intermediate solvent or resin affect glomerular basement membrane thickness? *Nephrology Dialysis Transplantation*, **24**, 400–403.

Ehrenreich, T. and Churg, J. (1968) Pathology of membranous nephropathy. *Pathology Annual*, **3**, 145–186.

Elhefnawy, N.G. (2011) Contribution of electron microscopy to the final diagnosis of renal biopsies in Egyptian patients. *Pathology and Oncology Research*, **17**, 121–125.

Estacio, R.O. and Schrier, R.W. (2001) Diabetic nephropathy: pathogenesis, diagnosis, and prevention of progression. *Advances in Internal Medicine*, **46**, 359–408.

Fattal, I., Shental, N., Mevorach, D. *et al.* (2010) An antibody profile of systemic lupus erythematosus detected by antigen microarray. *Immunology*, **130**, 337–343.

Furness, P. (2004) Paraproteinaemia and renal disease. *Current Diagnostic Pathology*, **10**, 52–60.

George, J.N. (2009) The thrombotic thrombocytopenic purpura and hemolytic uremic syndromes: overview of pathogenesis (Experience of The Oklahoma TTP-HUS Registry, 1989–2007). *Kidney International*, **75** (Suppl. 112), S8–S10.

Ghadially, F.N. (1988) *Ultrastructural Pathology of the Cell and Matrix*, 3rd edn, Butterworths, London.

Glassock, R.J. (2003) Secondary minimal change disease. *Nephrology Dialysis Transplantation*, **18** (Suppl. 6), vi52–vi58.

Gokden, N., Barlogie, B. and Liapis, H. (2008) Morphologic heterogeneity of renal light-chain deposition disease. *Ultrastructural Pathology*, **32**, 17–24.

Goldberg, S., Harvey, S.J., Cunningham, J. *et al.* (2009) Glomerular filtration is normal in the absence of both agrin and perlecan-heparan sulphate from

the glomerular basement membrane. *Nephrology Dialysis Transplantation*, **24**, 2044–2052.

Gregory, M.C. (2004) Alport syndrome and thin basement membrane nephropathy: unraveling the tangled strands of type IV collagen. *Kidney International*, **65**, 1109–1110.

Grimbert, P., Audard, V., Remy, P. *et al.* (2003) Recent approaches to the pathogenesis of minimal-change nephrotic syndrome. *Nephrology Dialysis Transplantation*, **18**, 245–248.

Gubler, M-C., Heidet, L. and Antignac, C. (2007) Alport's syndrome, thin basement membrane nephropathy, nail–patella syndrome, and type III collagen glomerulopathy, in *Heptinstall's Pathology of the Kidney*, 6th edn (eds J.C. Jennette, J.L. Olson, M.M. Schwartz and F.G. Silva), Lippincott Williams and Wilkins, Philadelphia, PA, pp. 487–515.

Haas, M. (2006) Thin glomerular basement membrane nephropathy: incidence in 3471 consecutive renal biopsies examined by electron microscopy. *Archives of Pathology and Laboratory Medicine*, **130**, 699–706.

Haas, M. (2007) Electron microscopy in renal biopsy interpretation – when and why we still need it. *US Nephrology*, **1** (1), 19–22.

Haas, M., Rajaraman, S., Ahuja, T. *et al.* (2000) Fibrillary/immunotactoid glomerulonephritis in HIV-positive patients: a report of three cases. *Nephrology Dialysis Transplantation*, **15** (10), 1679–1683.

Hammar, S.P., Luu, J., Bockus, D.E. *et al.* (1992) Induction of tubuloreticular structures in cultured human endothelial cells by recombinant interferon alpha and beta. *Ultrastructural Pathology*, **16**, 211–218.

Haraldsson, B., Nystrom, J. and Deen, W.M. (2008) Properties of the glomerular barrier and mechanisms of proteinuria. *Physiological Reviews*, **88**, 451–487.

Harvey, S.J., Jarad, G., Cunningham, J., Rops, A.L. *et al.* (2007) Disruption of glomerular basement membrane charge through podocyte-specific mutation of agrin does not alter glomerular permselectivity. *American Journal of Pathology*, **171**, 139–152.

Harvey, S.J., Zheng, K., Sado, Y. *et al.* (1998) Role of distinct type IV collagen networks in glomerular development and function. *Kidney International*, **54**, 1857–1866.

Hennigar, R.A. and Tumlin, J.A. (2009) Glomerular diseases associated primarily with asymptomatic or gross haematuria, in *Silva's Diagnostic Renal Pathology* (eds X.J. Zhou, Z. Laszik, T. Nadasdy *et al.*), Cambridge University Press, Cambridge, pp. 127–177.

Herrera, G.A. and Turbat-Herrera, E.A. (2010) Renal diseases with organized deposits: an algorithmic approach to classification and clinicopathologic diagnosis. *Archives of Pathology and Laboratory Medicine*, **134**, 512–531.

Herzenberg, A.M., Fogo, A.B., Reich, H.N. *et al.* (2011) Validation of the Oxford classification system of IgA nephropathy. *Kidney International*, **80**, 310–317.

Hsu, H-C. and Churg, J. (1979) Glomerular microfibrils in renal disease: a comparative electron microscopic study. *Kidney International*, **16**, 497–504.

Hudson, B.G., Tryggvason, K., Sundaramoorthy, M. and Neilson, E.G. (2003) Alport's syndrome, Goodpasture's syndrome and type IV collagen. *New England Journal of Medicine*, **348**, 2543–2556.

Ivanyi, B. and Degrell, P. (2004) Fibrillary glomerulonephritis and immunotactoid glomerulopathy. *Nephrology Dialysis Transplantation*, **19** (9), 2166–2170.

Jais, J.P., Knebelmann, B., Giatras, I. *et al.* (2000) X-linked Alport syndrome: natural history in 195 families and genotype–phenotype correlations in males. *Journal of the American Society of Nephrology*, **11** (4), 649–657.

Jais, J.P., Knebelmann, B., Giatras, I. *et al.* (2003) X-linked Alport syndrome: natural history and genotype–phenotype correlations in girls and women belonging to 195 families: a 'European Community Alport Syndrome Concerted Action' study. *Journal of the American Society of Nephrology*, **14**, 2603–2610.

Kalluri, R., Shield, C.F., Todd, P. *et al.* (1997) Isoform switching of type IV collagen is developmentally arrested in X-linked Alport syndrome leading to increased susceptibility of renal basement membranes to endoproteolysis. *Journal of Clinical Investigation*, **99** (10), 2470–2478.

Kiryluk, K., Gharavi, A.G., Izzi, C. and Scolari, F. (2010) IgA nephropathy – the case for a genetic basis becomes stronger. *Nephrology Dialysis Transplantation*, **25**, 336–338.

Kronz, J.D., Nue, A.M. and Nadasdy, T. (1998) When noncongophilic glomerular fibrils do not represent fibrillary glomerulonephritis: nonspecific mesangial fibrils in sclerosing glomeruli. *Clinical Nephrology*, **50** (4), 218–223.

LeBleu, V., Sund, M., Sugimoto, H. *et al.* (2010) Identification of the NC1 domain of $\alpha 3$ chain as critical for $\alpha 3\alpha 4\alpha 5$ type IV collagen network assembly. *The Journal of Biological Chemistry*, **285** (53), 41874–41885.

Lemmink, H.H., Mochizuki, T., van den Heuvel, L.P. *et al.* (1994) Mutations in the type IV collagen alpha 3 (COL4A3) gene in autosomal recessive Alport syndrome. *Human Molecular Genetics*, **3** (8), 1269–1273.

Leung, N., Lager, D.J., Gertz, M.A. *et al.* (2004) Long-term outcome of renal transplantation in light-chain deposition disease. *American Journal of Kidney Diseases*, **43** (1), 147–153.

Levy, M. and Feingold, J. (2000) Estimating prevalence in single-gene kidney diseases progressing to renal failure. *Kidney International*, **58** (3), 925–943.

Lin, J., Markowitz, G.S., Valeri, A.M. *et al.* (2001) Renal monoclonal immunoglobulin deposition disease: the disease spectrum. *Journal of the American Society of Nephrology*, **12**, 1482–1492.

Longo, I., Porcedda, P., Mari, F. *et al.* (2002) COL4A3/COL4A4 mutations: from familial hematuria to autosomal-dominant or recessive Alport syndrome. *Kidney International*, **61** (6), 1947–1956.

Markowitz, G.S., Cheng, J-T., Colvin, R.B. *et al.* (1998) Hepatitis C viral infection is associated with fibrillary glomerulonepritis and immunotactoid glomerulopathy. *Journal of the American Society of Nephrology*, **9**, 2244–2252.

Marquez, B., Stavrou, F., Zouvani, I. *et al.* (1999) Thin glomerular basement membranes in patients with hematuria and minimal change disease. *Ultrastructural Pathology*, **23**, 149–156.

Martin, P., Heiskari, N., Zhou, J. *et al.* (1998) High mutation detection rate in the COL4A5 collagen gene in suspected Alport syndrome using PCR and direct DNA sequencing. *Journal of the American Society of Nephrology*, **9** (12), 2291–2301.

Mathieson, P.W. (2003) Immune dysregulation in minimal change nephropathy. *Nephrology Dialysis Transplantation*, **18** (Suppl. 6), vi26–vi29.

Matignon, M., Cacoub, P., Colombat, M. *et al.* (2009) Clinical and morphological spectrum of renal involvement in patients with mixed cryoglobulinemia without evidence of hepatitis C infection. *Medicine*, **88**, 341–348.

McGrogan, A., Franssen, C.F.M. and de Vries, C.S. (2011) The incidence of primary glomerulonephritis worldwide: a systematic review of the literature. *Nephrology Dialysis Transplantation*, **26**, 414–430.

Meyrier, A.Y. (2009) Treatment of focal segmental glomerulosclerosis with immunophilin modulation: when did we stop thinking about pathogenesis? *Kidney International*, **76**, 487–491.

Miarka, P., Idzior-Waluś, B., Kuźniewski, M. *et al.* (2011) Corticosteroid treatment of kidney disease in a patient with familial lecithin–cholesterol acyltransferase deficiency. *Clinical and Experimental Nephrology*, **15**, 424–429.

Miller, C.A., Gattone, V.H. II, McLaughlin, H. *et al.* (2010) Identification of the NC1 domain of $\alpha 3$ chain as critical for $\alpha 3\alpha 4\alpha 5$ Type IV collagen network assembly. *Journal of Biological Chemistry*, 285 (53), 41874–41885.

Miner, J.H. (1998) Developmental biology of glomerular basement membrane components. *Current Opinion in Nephrology and Hypertension*, **7**, 13–19.

Mochizuki, T., Lemmink, H.H., Mariyama, M. *et al.* (1994) Identification of mutations in the alpha 3(IV) and alpha 4(IV) collagen genes in autosomal recessive Alport syndrome. *Nature Genetics*, **8** (1), 77–81.

Morita, T. and Churg, J. (1983) Mesangiolysis. *Kidney International*, **24**, 1–9.

Morita, M., White, R.H.R., Raafat, F. *et al.* (1988) Glomerular basement membrane thickness in children: a morphometric study. *Pediatric Nephrology*, **2**, 190–195.

Nasr, S.H., Markowitz, G.S., Valeri, A.M. *et al.* (2007) Thin basement membrane nephropathy cannot be diagnosed reliably in deparaffinized, formalin-fixed tissue. *Nephrology Dialysis Transplantation*, **22**, 1228–1232.

Nishi, S., Ueno, M., Hisaki, S. *et al.* (2000) Ultrastructural characteristics of diabetic nephropathy. *Medical Electron Microscopy*, **33**, 65–73.

Öqvist, B., Brenner, B.M., Oliveira, J.P. *et al.* (2009) Nephropathy in Fabry disease: the importance of early diagnosis and testing in high-risk populations. *Nephrology Dialysis Transplantation*, **24**, 1736–1743.

Patrakka, J. and Tryggvason, K. (2010) Molecular make-up of the glomerular filtration barrier. *Biochemical and Biophysical Research and Communications*, **396**, 164–169.

Pearson, J.M., McWilliam, L.J., Coyne, J.D. and Curry, A. (1994) Value of electron microscopy in the diagnosis of renal disease. *Journal of Clinical Pathology*, **47**, 126–128.

Pedchenko, V., Bondar, O., Fogo, A.B. *et al.* (2010) Molecular architecture of the Goodpasture autoantigen in anti-GBM nephritis. *New England Journal of Medicine*, **363**, 343–354.

Pescucci, C., Mari, F., Longo, I. *et al.* (2004) Autosomal-dominant Alport syndrome: natural history of a disease due to COL4A3 or COL4A4 gene. *Kidney International*, **65** (5), 1598–1603.

Ponticelli, C. (2010) Recurrence of focal segmental glomerular sclerosis (FSGS) after renal transplantation. *Nephrology Dialysis Transplantation*, **25**, 25–31.

Prunotto, M., Carnevale, M.L., Candiano, G. *et al.* (2010) Autoimmunity in membranous nephropathy targets aldose reductase and SOD2. *Journal of the American Society of Nephrology*, **21** (3), 507–519.

Rodríguez-Iturbe, B. and Batsford, S. (2007) Pathogenesis of poststreptococcal glomerulonephritis a century after Clemens von Pirquet. *Kidney International*, **71**, 1094–1104.

Rogers, T.E., Rakheja, D. and Zhou, X.J. (2009) Glomerular diseases associated with nephritic syndrome and/or rapidly progressive glomerulonephritis, in *Silva's Diagnostic Renal Pathology* (eds X.J. Zhou, Z. Laszik, T. Nadasdy *et al.*), Cambridge University Press, Cambridge, pp. 178–228.

Rosenstock, J.L., Markowitz, G.S., Valeri, A.M. *et al.* (2003) Fibrillary and immunotactoid glomerulonephritis: distinct entities with different clinical and pathologic features. *Kidney International*, **63**, 1450–1461.

Sanai, T., Okuda, S., Yoshimitsu, T. *et al.* (2007) Nodular glomerulosclerosis inpatients without any manifestation of diabetes mellitus. *Nephrology*, **12**, 69–73.

Sánchez-Corral, P. and Melgosa, M. (2010) Advances in understanding the aetiology of atypical haemolytic uraemic syndrome. *British Journal of Haematology*, **150**, 529–542.

Saus, J., Wieslander, J., Langeveld, J.P.M. *et al.* (1988) Identification of the Goodpasture antigen as the $\alpha 3$ (IV) chain of collagen IV. *Journal of Biological Chemistry*, **263** (26), 13374–13380.

Savige, J., Rana, K., Tonna, S. *et al.* (2003) Thin basement membrane nephropathy. *Kidney International*, **64**, 1169–1178.

Schwartz, M.M., Korbet, S.M. and Lewis, E.J. (2002) Immunotactoid glomerulopathy. *Journal of the American Society of Nephrology*, **13**, 1390–1397.

Siso, A., Ramos-Casals, M., Bové, A. *et al.* (2010) Outcomes in biopsy-proven lupus nephritis: evaluation of 190 white patients from a single centre. *Medicine*, **89** (5), 300–307.

Standeven, K.F., Ariëns, R.A.S. and Grant, P.J. (2005) The molecular physiology and pathology of fibrin structure/function. *Blood Reviews*, **19**, 275–288.

Sterzel, R.B., Lovett, H.D., Stein, H.D. and Kashgarian, M. (1982) The mesangium and glomerulonephritis. *Wiener Klinische Wochenschrift*, **60** (18), 1077–1094.

Stirling, J.W., Coleman, M., Thomas, A. and Woods, A.E. (2000) Role of transmission electron microscopy in tissue diagnosis: diseases of the kidney, skeletal muscle and myocardium. *Journal of Cellular Pathology*, **4** (4), 223–243.

Stokes, M.B., Nasr, S.H. and D'Agati, V.D. (2009) Systemic lupus erythematosus and other autoimmune diseases (mixed connective tissue disease, rheumatoid arthritis and Sjogren's syndrome), in *Silva's Diagnostic Renal Pathology* (eds X.J. Zhou, Z. Laszik, T. Nadasdy *et al.*), Cambridge University Press, Cambridge, pp. 229–272.

Strife, C.F., McEnery, P.T., McAdams, A.J. and West, C.D. (1977) Membranoproliferative glomerulonephritis with disruption of the glomerular basement membrane. *Clinical Nephrology*, **7** (2), 65–72.

Torra, R. (2008) Renal manifestations in Fabry disease and therapeutic options. *Kidney International*, **74** (Suppl. 111), S29–S32.

Venuturupalli, R.S. and Wallace, D.J. (2007) Lupus nephritis – an update. *Touch Briefings*, 63–66, http://www.touchbriefings.com/pdf/2968/wallace.pdf (accessed July 2012).

Vowles, G.H. (2008) Amyloid, in *Theory and Practice of Histological techniques*, 6th edn (eds J.D. Bancroft and M. Gamble), Churchill Livingstone Elsevier, Edinburgh, pp. 261–281.

Weening, J.J., D'Agati, V.D., Schwartz, M.M. *et al.* (2004) The classification of glomerulonephritis in systemic lupus erythematosus revisited. *Kidney International*, **65**, 521–530.

Wiggins, R.C. (2007) The spectrum of podocytopathies: a unifying view of glomerular diseases. *Kidney International*, **71**, 1205–1214.

Yang, Y., Hellmark, T., Zhao, J. *et al.* (2009a) Levels of epitope-specific autoantibodies correlate with renal damage in anti-GBM disease. *Nephrology Dialysis Transplantation*, **24**, 1838–1844.

Yang, A-H., Lin, B-S., Kuo, K-L. *et al.* (2009b) The clinicopathological implications of endothelial tubuloreticular inclusions found in glomeruli having histopathology of idiopathic membranous nephropathy. *Nephrology Dialysis Transplantation*, **24**, 3419–3425.

Yasuda, T., Imai, H., Nakamoto, Y. *et al.* (1992) Significance of fibrils in the formation of the Kimmelstiel–Wilson nodule. *Virchows Archives A: Pathological Anatomy and Histology*, **421**, 297–303.

Zhao, J., Cui, Z., Yang, R. *et al.* (2009) Anti-glomerular basement membrane autoantibodies against different target antigens are associated with disease severity. *Kidney International*, **76**, 1108–1115.